

1 **Aedes anphevirus (AeAV): an insect-specific virus distributed worldwide in *Aedes***
2 ***aegypti* mosquitoes that has complex interplays with *Wolbachia* and dengue virus**
3 **infection in cells**

4

5 Rhys Parry and Sassan Asgari*

6

7 Australian Infectious Disease Research Centre, School of Biological Sciences, The
8 University of Queensland, Brisbane, QLD 4072, Australia

9

10

11 **Running title:** Anphevirus from *Aedes aegypti*

12

13

14

15

16

17 **Word count (abstract):** 249

18 **Word count (importance):** 161

19 **Word count (text):** 5334

20

21

22

23

24

25

26

27 *Corresponding author: Sassan Asgari; Tel: +617 3365 2043; Fax: +617 3365 1655;
28 s.asgari@uq.edu.au

29

30 **Abstract**

31 Insect specific viruses (ISVs) of the yellow fever mosquito *Aedes aegypti* have been demonstrated
32 to modulate transmission of arboviruses such as dengue virus (DENV) and West Nile virus by the
33 mosquito. The diversity and composition of the virome of *Ae. aegypti*, however, remains poorly
34 understood. In this study, we characterised Aedes anphevirus (AeAV), a negative-sense RNA virus
35 from the order *Mononegavirales*. AeAV identified from *Aedes* cell lines were infectious to both *Ae.*
36 *aegypti* and *Aedes albopictus* cells, but not to three mammalian cell lines. To understand the
37 incidence and genetic diversity of AeAV, we assembled 17 coding-complete and two partial
38 genomes of AeAV from available RNA-Seq data. AeAV appears to transmit vertically and be
39 present in laboratory colonies, wild-caught mosquitoes and cell lines worldwide. Phylogenetic
40 analysis of AeAV strains indicates that as the *Ae. aegypti* mosquito has expanded into the
41 Americas and Asia-Pacific, AeAV has evolved into monophyletic African, American and Asia-
42 Pacific lineages. The endosymbiotic bacterium *Wolbachia pipientis* restricts positive-sense RNA
43 viruses in *Ae. aegypti*. Re-analysis of a small RNA library of *Ae. aegypti* cells co-infected with
44 AeAV and *Wolbachia* produces an abundant RNAi response consistent with persistent virus
45 replication. We found *Wolbachia* enhances replication of AeAV when compared to a tetracycline
46 cleared cell line, and AeAV modestly reduces DENV replication *in vitro*. The results from our study
47 improve understanding of the diversity and evolution of the virome of *Ae. aegypti* and adds to
48 previous evidence that shows *Wolbachia* does not restrict a range of negative strand RNA viruses.

49 **Importance**

50 The mosquito *Aedes aegypti* transmits a number of arthropod-borne viruses (arboviruses) such as
51 dengue virus and Zika virus. Mosquitoes also harbour insect-specific viruses that may affect
52 replication of pathogenic arboviruses in their body. Currently, however, there are only a handful of
53 insect-specific viruses described from *Ae. aegypti* in the literature. Here, we characterise a novel
54 negative strand virus, Aedes anphevirus (AeAV). Meta-analysis of *Ae. aegypti* samples showed
55 that it is present in *Ae. aegypti* mosquitoes worldwide and
56 is vertically transmitted. *Wolbachia* transinfected mosquitoes are currently being used in biocontrol
57 as they effectively block transmission of several positive sense RNA viruses in mosquitoes. Our

58 results demonstrate that *Wolbachia* enhances the replication of AeAV and modestly reduces
59 dengue virus replication in a cell line model. This study expands our understanding of the virome in
60 *Ae. aegypti* as well as providing insight into the complexity of the *Wolbachia* virus restriction
61 phenotype.

62 **Introduction**

63 The yellow fever mosquito *Aedes aegypti* is a vector of medically important viruses with worldwide
64 distribution within the tropical and subtropical zones (1). *Ae. aegypti* is the principal vector of both
65 dengue virus (DENV) and Zika virus (ZIKV) (Family: *Flaviviridae*) with estimates suggesting up to
66 390 million incidences of DENV infections a year (2), and approximately 400,000 cases of ZIKV
67 during the 2015–2016 Latin American ZIKV outbreak (3).

68 The ability of mosquitoes to transmit viruses is determined by a complex suite of genetic and
69 extrinsic host factors (4-6). One developing area is the contribution of insect-specific viruses
70 (ISVs), demonstrated not to replicate in mammalian cells, in the vector competence of individual
71 mosquitoes (7, 8). ISVs can suppress the anti-viral RNAi response as shown in *Culex*-Y virus
72 (CYV) of the *Birnaviridae* family (9), or enhance the transcription of host factors; cell fusing agent
73 virus (CFAV) (Family: *Flaviviridae*) infection of *Ae. aegypti* Aa20 cells upregulates the V-ATPase-
74 associated factor RNASEK allowing more favourable replication of DENV (10). ISVs have also
75 been shown to suppress or exclude replication of arboviruses; prior infection of *Aedes albopictus*
76 C6/36 cells and *Ae. aegypti* mosquitoes with Palm Creek virus (PCV) (Family: *Flaviviridae*) has
77 been shown to suppress replication of the zoonotic West Nile virus (WNV) and Murray Valley
78 encephalitis virus (Family: *Flaviviridae*) (11, 12). Also, it has recently been demonstrated in *Aedes*
79 cell lines that dual infection with Phasi Charoen-like virus (Family: *Bunyaviridae*) and CFAV
80 restricts the cells permissivity to both DENV and ZIKV infection (13).

81 Metagenomic and bio-surveillance strategies have proved invaluable in describing the virome
82 diversity of wild-caught *Culicinae* mosquitoes (14, 15). To date, six ISVs have been identified and
83 characterised from wild-caught and laboratory *Ae. aegypti*; CFAV (16, 17), Phasi Charoen-like
84 virus (Family: *Bunyaviridae*) (18), Dezidougou virus from the Negevirus taxon (19), *Aedes*
85 densovirus (Family: *Parvoviridae*) (20) and the unclassified Humaita-Tubiaca virus (HTV)

86 (21). Recently, transcriptomic analysis of wild-caught *Ae. aegypti* mosquitoes from Bangkok,
87 Thailand and Cairns, Australia suggested possible infection of the mosquitoes with up to 27 insect-
88 specific viruses, the majority of which currently uncharacterized (22). This represents a narrow
89 understanding of the diversity of the circulating virome harboured by *Ae. aegypti* mosquitoes.

90 In this study, we identified and characterised a novel negative-sense RNA *Anphevirus*, putatively
91 named *Aedes anphevirus* (AeAV), from the order *Mononegavirales* in *Ae. aegypti* mosquitoes.
92 According to the most recent International Committee on Taxonomy of Viruses (ICTV) report (23),
93 Xīnchéng mosquito virus (XcMV), assembled as part of a metagenomic analysis of *Anopheles*
94 *sinensis* mosquitoes in Xīnchéng China, is the only member of the *Anphevirus* genus and closely
95 related to members of *Bornaviridae* and *Nyamiviridae* (24). Originally thought to only encode for
96 four ORFs, presence of a number of closely related viruses to XcMV from West African *Anopheles*
97 *gambiae* mosquitoes (15) and West Australian *Culex* mosquitoes (25) suggests that members of
98 this taxon encode for six ORFs with a genome size of approximately 12kb.

99 The endosymbiotic bacterium *Wolbachia pipientis* was first shown to restrict RNA viruses in
100 *Drosophila melanogaster* (26, 27). Transinfection of *Wolbachia* into *Ae. aegypti* restricted DENV
101 and Chikungunya virus (Family: *Togaviridae*) replication in the host (28). In *Ae. aegypti* Aag2 cells,
102 stably transfected with a proliferative strain of *Wolbachia* (wMelPop-CLA), the endosymbiont
103 restricts CFAV (29), but has no effect on the negative sense Phasi Charoen-like virus (Family:
104 *Bunyaviridae*) (30). In addition to characterising AeAV, we also studied the effect of *Wolbachia* on
105 AeAV replication and co-infection of AeAV and DENV in *Ae. aegypti* cells.

106 **Results**

107 **Identification and assembly of the full *Aedes anphevirus* (AeAV) genome from *Wolbachia*-** 108 **infected *Aedes* cells**

109 During replication of RNA viruses in *Ae. aegypti* mosquitoes, the RNA interference (RNAi) pathway
110 cleaves viral dsRNA intermediates into 21nt short interfering RNAs (vsiRNAs) (31, 32). Using this
111 fraction of reads from RNA-Seq data, it is possible to *de novo* assemble virus genomes (21, 33).

112 The previously sequenced small RNA fraction of embryonic *Ae. aegypti* Aag2 cells and Aag2 cells
113 stably infected with *Wolbachia* (wMelPop-CLA strain) (34) was trimmed of adapters, filtered for
114 21nt reads and *de novo* assembled using CLC Genomics Workbench with a minimum contig
115 length of 100nt. The resulting contigs were then queried using BLASTX against a local virus
116 protein database downloaded from the National Centre for Biotechnology Information (NCBI). In
117 the Aag2.wMelPop-CLA assembly, four contigs between 396-1162nt were found to have amino
118 acid similarity (E value 9.46E-51) to proteins from two closely related *Mononegavirales* viruses:
119 *Culex mononega-like virus 1* (CMLV-1) and *Xīnchéng mosquito virus* (XcMV); the type species for
120 the *Anphevirus* genus. No contigs from the *Wolbachia* negative *Ae. aegypti* Aag2 dataset showed
121 any similarity to CMLV-1 or XnMV.

122 Subsequent RT-PCR analysis between RNA samples from Aag2 and Aag2.wMelPop-CLA cell
123 lines indicated that this tentative virus was exclusive to the Aag2.wMelPop-CLA cell line (Fig. 1A).
124 We hypothesised that the presence of any putative virus may have been the result of
125 contamination during *Wolbachia* transinfection. The *Wolbachia* wMelPop-CLA strain was isolated
126 from the *Ae. albopictus* cell line RML-12 and transinfected into Aag2 (35) and the *Ae. albopictus*
127 C6/36 (C6/36.wMelPop-CLA) cell lines (36). RT-PCR analysis of RNA extracted from RML-12 and
128 C6/36 cells, as well as the *Ae. aegypti* cell line Aa20, showed that the putative virus was present
129 only in RML-12 cells (Fig. 1A).

130 To recover the remainder of the virus genome, transcriptome RNA-Seq data from RML-
131 12.wMelPop-CLA and C6/36.wMelPop-CLA cells were downloaded (37, 38) and *de novo*
132 assembled with automatic bubble and word sizes using CLC Genomics Workbench. BLASTN
133 analysis of assembled contigs indicated that a complete 12,940 contig from the C6/36.wMelPop-
134 CLA cells and two contigs (9624 and 3487nt) from RML-12.wMelPop-CLA were almost identical
135 (99-100% pairwise nucleotide identity) to the virus like contigs assembled from Aag2.wMelPop-
136 CLA. We were then able to use this reference to recover the full genomes from Aag2.wMelPop-
137 CLA and RML-12.wMelPop-CLA consensus mapping to this reference. To re-validate that AeAV
138 was only present in Aag2.wMelPop-CLA cells, reads from the *Wolbachia*-negative Aag2 cells were
139 mapped to the representative genome, and only four reads were identified in the data. The result

140 from here and the RT-PCR analysis above (Fig. 1A) also confirm that the virus found in the
141 *Wolbachia* transinfected cells originate from RML-12 cells in which wMelPop-CLA was originally
142 transinfected and subsequently transferred to other cell lines.

143 **Characterisation of Aedes anphevirus (AeAV)**

144 AeAV genomes assembled in this study were between 12,455 to 13,011 nucleotides in length with
145 a %GC content of 46.8% and encode for 7 non-overlapping ORFs (Fig. 1B). Phylogenetic analysis
146 of the RNA-dependent RNA polymerase protein places AeAV within a well-supported clade of the
147 unassigned *Anphevirus* genus, which are from the order *Mononegavirales* and closely related to
148 members of *Bornaviridae* and *Nyamiviridae* (Fig. 1C).

149 All members of *Mononegavirales* have a negative-stranded RNA genome encapsidated within the
150 capsid and the RNA polymerase complex (39). The RNA genome is used as the template by the
151 RNA polymerase complex to sequentially transcribe discrete mRNAs from subgenomic genes.
152 mRNA from each gene is capped and polyadenylated. To analyse the transcriptional activity of
153 AeAV, we used the poly-A enriched RNA-Seq libraries prepared from the Cali, Colombia laboratory
154 strain (40). Read mapping and coverage analysis of the AeAV genome showed that AeAV follows
155 the trend of reduced transcriptional activity seen in other *Mononegavirales* species (41) with
156 approximately 50% reduction between ORF1 and ORF2 but an increased transcription between
157 ORF2 and ORF3 (Fig. 1B). The reduction in transcriptional activity of AeAV genes is conserved for
158 each sequential ORF with the least transcriptional activity for ORF7/L protein, that is conserved in
159 all AeAV strains in Poly(A) enriched RNA-Seq libraries (Fig. S1).

160 ORF1 of AeAV encodes a predicted 49kDa nucleoprotein with no transmembrane domains and
161 closest pairwise amino acid identity (26%) to the nucleoprotein gene from *Culex mononega*-like
162 virus 1 (CMLV-1) from *Culex* mosquitoes in Western Australia (25). Protein homology analysis
163 using HHPred showed that ORF1 was a likely homolog of the p40 nucleoprotein of the Borna
164 disease virus (Probability 98.66%, E- value: 7.1e-10). ORF2 encodes an 11kDa protein with two
165 transmembrane domains in the N-terminus of the protein with no similarity to any proteins within
166 the non-redundant protein database or homologs as predicted by HHPred. ORF3 and ORF4
167 encode putative glycoproteins, 64kDa and 72kDa, respectively. ORF3 has no pairwise amino acid

168 similarity to any virus protein or homologs as per HHPred analysis. ORF4 was predicted to have a
169 signal peptide in the N-terminus followed by a heavily O- and N-linked glycosylated outside region
170 as well as two transmembrane domains in the C-terminus of the protein. ORF4 is most closely
171 related to the glycoprotein from the Gambie virus identified from West African *An. gambiae*
172 mosquitoes with 45% pairwise amino acid identity (15). Protein homology analysis predicted ORF4
173 to be a homolog of the Human Herpesvirus 1 Envelope Glycoprotein B (Probability 99.88%, E-
174 value 2.2e-22).

175 The presence of a Zinc-like finger (ZnF) domain in a small ORF proximal to the L protein previously
176 reported in closely related viruses (15) (Fig. 2A and B), was identified in AeAV based on sequence
177 alignment (Fig. 1B). Re-analysis of putative ORFs from CMLV-1 and CMLV-2 (25) showed the
178 presence of this GATA-like ZnF domain in both of these viruses and the genus type species XcMV
179 identified from *An. sinensis* (24) (Fig. 2C).

180 ORF6 encodes for a small 4kDa protein that has a single transmembrane domain in the C-
181 terminus. This protein was almost missed in the prediction of ORFs due to having only 37 amino
182 acids, however, it has a strong transcriptional coverage in Poly-A datasets and exists in all
183 assembled strains (Fig. 1B and Fig. S1). It was predicted to share no structural homology or amino
184 acid identity with any previously reported peptide. In addition to this, we were able to identify small
185 transmembrane domain containing proteins proximal to or overlapping with the ZnF protein in
186 CMLV-1, CMLV-2 and XcMV (Fig. 2A), suggesting that this protein may be a conserved feature of
187 anpheviruses.

188 ORF7 encodes for the 226kDa L protein, has 41% pairwise amino acid identity with the RNA
189 dependent RNA polymerase from CMLV-1. Protein domain analysis of the L protein showed the
190 highly conserved *Mononegavirales* RNA dependent RNA polymerase, mRNA capping domain and
191 a mRNA (guanine-7-) methyltransferase (G-7-MTase) domain conserved in all L proteins in
192 *Mononegavirales* (42).

193 **AeAV cis-regulatory elements**

194 For identification of *cis*-regulatory elements in the AeAV genome, we used MEME (Multiple Em for
195 Motif Elicitation) to search for overrepresented 5-50nt motifs (43). Using a 0-order Markov model,
196 one 32nt motif 3'-UUVCUHWUAAAAAACCCGCGYAGUUASAAAUCA-5' was considered statistically
197 significant (E-value: 4.2e-010). Importantly the motif was proximal to each predicted virus gene
198 ORF, suggesting it may be a potential promoter (Fig. 3A and C). No motif was found between ORF
199 5 and 6 in AeAV suggesting that these two genes may be under the control of a single *cis*-
200 regulatory element. Interestingly, the complement of this motif appeared twice on the anti-genome
201 suggesting that it may be used in an anti-genome virus intermediate. We noticed that these motifs
202 localised to partial palindromic repeats and predicted that they may form stable secondary RNA
203 structures. Using RNAfold, we were able to visualise and predict the MFE structure 20nt upstream
204 and downstream of the motif (44). All predicted *cis*-regulatory motifs formed partial or complete
205 stable secondary stem loops and hairpins with high base-pair probabilities (Fig. 3B). The exception
206 was predicted element 3, which is proximal to the second ORF; as this second gene is transcribed
207 less than ORF3 irrespective of its similarity to the motif, the lack of a stable stem loop structure
208 may be a novel transcriptional regulatory mechanism. The presence of two conserved
209 homopolymeric triplets in the overrepresented motif is very similar to "slippery" -1 ribosome frame
210 shifting (RFS) sites XXX YYY Z (X=A, G, U; Y=A, U; Z=A, C, U) (45). It has been previously
211 demonstrated that similar 'slippery' sequence motifs followed by a predicted stem-loop structure is
212 a feature of rhabdovirus gene overlap regions (46). In AeAV, this feature appears in the intergenic
213 space and is unlikely to represent ribosomal frame shifting event and subsequent extension of a
214 protein. We also searched for additional slippery motifs in the AeAV genome. The genomic context
215 for each predicted "slippery motif" did not extend or produce additional ORFs.

216 **AeAV infection is widespread in *Ae. aegypti* laboratory colonies, wild-caught mosquitoes** 217 **and cell lines**

218 Taking advantage of the currently published RNA-Seq data, we performed a meta-analysis of
219 global incidence and genetic diversity of this virus. We were able to show that AeAV is ubiquitous
220 in laboratory colonies, cell lines and wild-caught *Ae. aegypti* mosquitoes. During preparation of this
221 manuscript a partial AeAV genome of 5313nt (Accession: MG012486.1) was deposited into NCBI

222 nucleotide database from a study characterising the evolution of piRNA pathways across
223 arthropods (47). Using our AeAV genome reference, we were able to complete the CDS portion of
224 the genome and also 16 additional strains of AeAV with two additional incomplete genomes (Fig.
225 4) (Table S1).

226 AeAV was present in colonies of *Ae. aegypti* established from eggs collected in Bakoumba, Gabon
227 (48) and also from Rabai, Kenya (designated K2, K14) as well as four mated hybrid strains (49). In
228 colonies wild caught from locations in the Americas (47), full genomes of AeAV were assembled
229 from Miami, USA , Cali, Colombia (40), and Chetumal, Mexico (50, 51) laboratory strains. Partial
230 genomes of AeAV were assembled from Cayenne and St-Georges, French Guiana (52). AeAV
231 was identified in colonies established from eggs collected in Chaiyaphum and Rayong, Thailand
232 (49, 53) as well as Jinjang, Malaysia (54). AeAV was also identified from the widely used Bora-
233 Bora reference strain from French Polynesia (55). AeAV was also present in eight pools of wild-
234 caught *Ae. aegypti* mosquitoes used for ZIKA bio-surveillance in Miami, Florida (56) as well as
235 Nakhon Nayok, and Bangkok, Thailand (18, 22).

236 In *Aedes* cell lines, AeAV was assembled from RNA-Seq data from the larval *Ae. aegypti* line CCL-
237 125 originally produced in Pune, India (57) and sequenced by the Arthropod Cell Line RNA-Seq
238 initiative, Broad Institute (broadinstitute.org). With the exception of RNA-Seq data from the three
239 *Aedes* cell lines stably infected with *Wolbachia* (RML-12.wMelPop-CLA, C6/36.wMelPop-CLA and
240 Aag2.wMelPopCLA), AeAV was not identified in any other available C6/36 or Aag2 RNA-Seq
241 libraries.

242 **Genetic variation and evolution of AeAV strains**

243 To assess relatedness and evolution between AeAV strains, a Maximum likelihood phylogeny
244 (PhyML) was undertaken of the CDS region of all strains with complete genomes (Fig. 5A). The
245 unrooted radial phylogenetic tree indicated three strongly supported monophyletic lineages
246 associated with the geographic origin of the sample. We have designated these lineages of AeAV
247 as African, American and Asia-Pacific (Fig. 5B).

248 In the American lineage of AeAV, all strains that are associated with *Wolbachia*-infected *Aedes* cell
249 lines (RML-12.wMelPop-CLA, C6/36.wMelPop-CLA and Aag2.wMelPopCLA) are almost identical
250 (99.55-99.86% identity), supporting the hypothesis that contamination of C6/36 and Aag2 cell lines
251 infected with *Wolbachia* is likely from the original RML-12 cell line. AeAV from the eight wild-caught
252 pools of *Ae. aegypti* mosquitoes from Florida, USA (56) and the laboratory colony established from
253 wild collected samples Florida (47) were almost identical (99.86% pairwise identity) with only 17nt
254 differences over the CDS region. The three African lineage strains of AeAV were slightly closer in
255 pairwise nucleotide identity to the American strains (92.65-93.15%) than the Asia/Pacific strains
256 (91.63%-91.74%). All samples that originated from Thailand form a monophyletic group and are
257 closely related to other Thai strains (99.23-99.62%).

258 We hypothesised that AeAV may have been harboured as part of the virome of *Ae. aegypti*
259 mosquitoes as *Ae. aegypti* expanded from its sub-Saharan African location into the Americas and
260 Asia-Pacific (58). Phylogenetic studies of the *Ae. aegypti* genome support the origin of *Ae. aegypti*
261 from Africa into the New World (Americas) and a subsequent secondary invasion of *Ae. aegypti*
262 *aegypti* from the New World to the Asia-Pacific region (59, 60). Comparing the evolution of the *Ae.*
263 *aegypti* nuclear genome with the evolution of AeAV indicates that the Asia-Pacific strains of AeAV
264 have not evolved from the currently circulating American strain lineage. This may indicate that the
265 virus was established independently in both the New-world Americas and also in the Asia-Pacific
266 (Fig. 5B).

267 **Anphevirus-like insertions into the *Ae. aegypti* genome**

268 The *Ae. aegypti* genome has a large repertoire of virus genes and partial viral genomes, termed
269 Endogenous Viral Elements (EVEs) (61, 62). To explore the possibility of anphevirus-like insertions
270 within the *Ae. aegypti* genome, we queried the most recent Liverpool genome (Aaegl5) with the
271 Aag2.wMelPop-CLA AeAV reference strain using the VectorBase BLASTN suite
272 (<https://www.vectorbase.org/blast>). There were numerous hits of nucleotide similarity (67-70%) of
273 500-1704nt regions dispersed throughout the *Ae. aegypti* genome. EVEs are acquired through
274 recombination with long terminal repeat (LTR) retrotransposons (62). We present one ~20kb
275 portion of Chromosome 2 of the *Ae. aegypti* genome (Fig. 6) with four anphevirus-like insertions

276 and close proximity to LTR retrotransposable fragments in unidirectional orientation. This suggests
277 insertion of viral elements through LTR retrotransposases and a long evolutionary history of
278 challenge with anphevirus-like species in *Ae. aegypti*.

279 ***Aedes Anphevirus (AeAV) replicates in Aedes cell lines but does not replicate in three*** 280 ***mammalian cell lines***

281 Supernatant of Aag2.ϖMelPop-CLA cells was infectious to both *Ae. aegypti* cells (Aa20), and *Ae.*
282 *albopictus* C6/36 cells over a five-day time course through RT-qPCR analysis (Fig. 7A). Generally,
283 there was significantly more relative AeAV genome copies detected in C6/36 cells at 1 and 5 dpi
284 compared to Aa20 cells. There were also significantly more anti-genome copies of AeAV in C6/36
285 cells over the five-day time course. The higher replication of AeAV in C6/36 cells as compared to
286 Aa20 cells is not unexpected since C6/36 cells are RNAi deficient and generally RNA viruses
287 replicate more efficiently in the cells (63-65).

288 We assumed that AeAV is an insect-specific virus based on its phylogenetic position, however, to
289 test if AeAV can replicate in mammalian cells, we inoculated human hepatocellular carcinoma cells
290 (Huh-7), African green monkey cells (Vero), and baby Hamster Kidney (BSR) cells with medium
291 from AeAV-infected cells and performed RT-PCR for AeAV RNA genome abundance over a 7-day
292 time course. While AeAV RNA (most likely from the inoculum) could be detected by RT-PCR at
293 day 1 and 3 after inoculation, it did not increase over time and was visibly reduced in the
294 mammalian cells by 5/7 dpi (Fig. 7B). AeAV was also not detected in the *An. gambiae* cell line
295 MOS-55 transfected with ϖMelPop-CLA from RML-12-ϖMelPop-CLA (36) sequenced by the
296 Arthropod Cell Line RNA-Seq initiative, Broad Institute (broadinstitute.org). Taken together, the
297 results suggest that AeAV infection may be restricted within the subfamily *Culicinae* or even the
298 *Aedes* genus and is insect specific.

299 ***Wolbachia pipientis* infection in *Ae. aegypti* cells enhances AeAV replication**

300 As *Wolbachia* is being deployed in the field to reduce dengue transmission, we were interested to
301 find out if it has any effect on replication of AeAV. We extracted RNA from Aag2.ϖMelPop-CLA
302 cells and a previously tetracycline cured Aag2.ϖMelPop-CLA cell line (66), and tested the effect of

303 *Wolbachia* infection on AeAV genome and anti-genome copies. AeAV genomic RNA copies were
304 significantly greater in *Wolbachia*-infected (Aag2.ϖMelPop-CLA) cells than those in tetracycline
305 cleared (Aag2.ϖMelPop-CLA.Tet) *Ae. aegypti* cells, however, there was no statistically significant
306 difference between the relative anti-genome copies between the two cell lines (Fig. 8A).

307 To explore the host small RNA response to AeAV, clean reads from previously prepared sRNA
308 libraries from Aag2.ϖMelPop-CLA and Aag2 (34) were mapped to the AeAV genome. In the
309 cytoplasmic fraction of the Aag2.ϖMelPop-CLA sample 870,012 of 4,686,954 reads (18.56%)
310 mapped to AeAV. In the nuclear fraction 420,215 of 11,406,324 reads (3.68%) mapped to the
311 genome. In the combined Aag2 sRNA library, of 8,600,821 clean reads only four reads mapped to
312 the AeAV genome. The mapping profile of 18-31nt reads mapped from the Aag2.ϖMelPop-CLA
313 library to AeAV indicates a higher proportion 27–31nt viral derived PIWI RNAs (vpiRNAs) than the
314 21nt vsiRNAs (Fig. 8B).

315 Analysis of the profile of mapped AeAV vsiRNAs fairly ubiquitously targeted the AeAV genome and
316 anti-genome (Fig. 8C). Hotspots in the vpiRNA mapping profile appeared to target the 3'UTR and
317 ORF1 and the 5'UTR of the AeAV anti-genome (Fig. 8D). Biogenesis of vpiRNAs are independent
318 of Dicer-2 with a bias for adenosine at position 10 in the sense position and a uracil in the first
319 nucleotide of antisense polarity (67). This “ping-pong” characteristic signature was apparent in the
320 vpiRNA reads from the cell line (Fig. 8E and F).

321 **Persistent infection of AeAV in Aa20 cells modestly reduces replication of DENV-2 genomic** 322 **RNA**

323 Recently, it has been demonstrated that in *Aedes* cell lines experimentally infected with two ISVs
324 replication of DENV and ZIKV was reduced (13). To test if there was any interaction between
325 AeAV and the subsequent challenge of cells with DENV, we generated an Aa20 cell line inoculated
326 with medium from RML-12 and maintained it for three passages. Aa20 cells persistently infected
327 with AeAV were challenged with 0.1 and 1 multiplicities of infection (MOI) of DENV-2 ET-100
328 strain. RT-qPCR analysis of DENV-2 genomic RNA showed that accumulation was on average
329 less in AeAV infected Aa20 cells as compared to the control (Fig. 9A and B). This reduction in
330 DENV-2 genome copies was statistically significant at MOI of 0.1 at both three and five days post

331 infection. No AeAV-related RT-qPCR product was detected in mock-infected Aa20 cells (data not
332 shown). We also examined the effect of DENV infection on AeAV RNA levels in the AeAV
333 persistently infected cells. RT-qPCR analysis showed no significant effect on AeAV levels between
334 1 and 3 days post-DENV infection, however, AeAV genomic RNA levels significantly declined at 5
335 days-post DENV infection (Fig. 9C). There was no significant difference in the results between 0.1
336 and 1 MOI of DENV.

337 **Evidence for vertical transmission of AeAV**

338 We were fortunate to explore the potential vertical transmission of AeAV by using RNA-Seq data of
339 uninfected and infected mated individuals from a study characterising the genetic basis of olfactory
340 preference in *Ae. aegypti* (49). Briefly, McBride and colleagues used eggs from a number of *Ae.*
341 *aegypti* species in Rabai, Kenya to establish laboratory colonies for RNA-Seq analysis. We
342 identified AeAV in the domestic K2 and K14 colonies, which was seemingly absent from the other
343 Rabai (K18, K19, K27) colonies. The K27 colony was interbred with the strain K14, which we found
344 to be AeAV positive. In all the four resultant hybrid colonies, which were subjected to RNA-Seq
345 analysis, we were able to *de novo* assemble identical K14 AeAV strain genomes (Fig. 10).

346 The possibility of vertical transmission also is supported by the presence of AeAV in both RNA-Seq
347 data from the sperm of adult male mosquitoes (54) and the female reproductive tract (53).

348 **Discussion**

349 The ability of AeAV to propagate in *Ae. aegypti* and *Ae. albopictus* cell lines but not in the three
350 mammalian cell lines suggests that AeAV is most likely an ISV, although this needs to be further
351 confirmed using cell lines from other species. To the best of our knowledge, this is the first
352 comprehensive characterisation of any *Anphevirus* species within *Mononegavirales* and the first
353 *Mononegavirales* virus species within *Ae. aegypti*. Although as this manuscript was under revision,
354 the complete genome sequence of AeAV and its phylogenetic relationship with other ISVs was
355 published in a short communication (68). While we have demonstrated that AeAV is spread
356 worldwide in *Ae. aegypti* mosquitoes, we have limited understanding as to how prevalent AeAV is
357 in individual mosquitoes in wild populations, its tissue tropism, or potential impacts on the host.

358 Although it is likely that AeAV is maintained in wild populations of *Ae. aegypti* mosquitoes through
359 vertical transmission, it is possible that AeAV could be maintained through venereal transmission as
360 we were able to identify the whole AeAV genome from a dataset prepared from the sperm of adult
361 male *Ae. aegypti* mosquitoes (54).

362 To our knowledge, the oldest continually maintained colony of laboratory mosquitoes with AeAV
363 present comes from Jinjang, Malaysia, which was established from wild-collected samples from as
364 early as 1975 (54). This suggests vertical transmission rates of AeAV are high or a high incidence
365 of AeAV within the colony. In comparison, in both French Guiana colonies, we were unable to
366 recover the complete genomes from these strains. It is unlikely that this is due to insertion of AeAV
367 into the nuclear *Ae. aegypti* genome as numerous reads mapped to the ORF7/L region of the
368 reference strain; however, there was not enough coverage to reach consensus of the full genome.
369 As these libraries were prepared from homogenates of mosquitoes, it seems likely that the
370 incidence of infection within these colonies may be lower; however, further analysis would have to
371 be conducted.

372 In our analysis, AeAV was not detected in any of the widely used Liverpool (LVP) and
373 Rockefeller/UGAL, as well as derived “white eye mutant” strains of *Ae. aegypti*. Analysis of
374 published ncRNA-Seq data from Australian Townsville and Cairns colonies of wild-caught
375 Australian mosquitoes (69, 70) suggests that there is no RNAi response or presence of AeAV in
376 these mosquitoes. Evidence from this study and others suggests that widely used laboratory
377 strains of *Ae. aegypti* harbour a diverse and heterogeneous virome composition and may
378 contribute to the variable vector competence between these colonies.

379 In our analysis, the geographic origin of the RNA-Seq samples matched the resulting phylogenetic
380 relationship of each strain. The presence of AeAV in the *Ae. albopictus* cell line RML-12,
381 presumably the origin of the AeAV contamination in other *Aedes* cell lines transfected with
382 adapted *wMelPop* strain, was the only *Ae. albopictus* sample in our analysis. During our analysis,
383 we queried all of the 266 currently available *Ae. albopictus* RNA-Seq datasets (TaxonID: 7160)
384 uploaded to the SRA, none of which indicated presence of AeAV. We hypothesise that AeAV from
385 RML-12 is likely due to contamination as the cell line is often mischaracterised as originating from

386 *Ae. aegypti* (71, 72). In many laboratories that study arbovirus interactions, more than one *Aedes*
387 cell line is maintained. As the RML-12 AeAV strain is genetically placed within the American
388 lineage, and the namesake of the cell line, Rocky Mountain Laboratories, (71) located in Montana,
389 USA suggests possible contamination from domestic *Ae. aegypti* mosquito samples. While no
390 other *Ae. albopictus* RNA-Seq data were positive for AeAV in this study, we cannot rule out the
391 possibility that AeAV could exist in American populations of *Ae. albopictus*. *Ae. aegypti* and *Ae.*
392 *albopictus* co-exist in North America and compete for larval habitats of discarded tires and other
393 artificial containers (73).

394 RNAi response is commonly observed in mosquitoes against RNA viruses. This response includes
395 miRNA, siRNA and piRNA pathways (74, 75). Similarly, we found a large number of 21nt vsiRNAs
396 produced against AeAV in infected cells that were evenly mapped to both sense and antisense
397 strands, indicating that dsRNA intermediates produced during replication must be the target of the
398 host cell RNAi response. In addition, a large number of vpiRNAs were found mapped to the 5'UTR,
399 ORF1 and the 3'UTR of the AeAV genome. These vpiRNAs had the typical ping-pong signature
400 (U₁-A₁₀) of secondary piRNAs. This signature has also been found in vpiRNAs produced during
401 alphavirus (76) and bunyavirus (63, 77) infections, but not in vpiRNA-like small RNAs in most
402 flaviviruses, such as DENV (78), ZIKV (79, 80) and an insect-specific flavivirus (81). We found a
403 higher proportion of small RNAs from Aag2-*wMelPop-CLA* cells that mapped to AeAV are vpiRNAs
404 (about 50%) as compared to less than 10% vsiRNAs. Literature suggests that when the siRNA
405 pathway is compromised more vpiRNAs are produced. This has been shown in RNAi deficient
406 C6/36 cells when infected with Sindbis virus, Rift Valley fever virus or La Crosse virus (63-65). The
407 RNA-Seq data from C6/36.*wMelPop-CLA* cells were for long transcripts rather than small RNAs,
408 therefore we were not able to confirm if in those cells there are higher proportion of vpiRNAs than
409 vsiRNAs. The over-representation of vpiRNAs in respect to vsiRNAs has also been demonstrated
410 in negative-sense *Bunyavirales* members PCLV and RVFV (30, 65) in Aag2 cells for all segments
411 of the genome. It remains to be seen however if the higher vpiRNA to vsiRNA ratio in
412 Aag2.*wMelPop-CLA* could be due to suppression of the siRNA pathway by AeAV, or alternatively,
413 *Wolbachia* may have an effect on the siRNA pathway. It seems however more likely that as

414 negative sense RNA viruses produce less dsRNA replicative intermediates, these could be simply
415 less targeted by the siRNA pathway and are unable to be resolved by sRNA profiling. These
416 possibilities require further investigations, and it remains to determine the role of the vpiRNAs in
417 AeAV replication or host anti-viral response.

418 The effects of *Wolbachia* on virus restriction are variable and depend on *Wolbachia* strain, virus
419 family and transinfected host (82). *Wolbachia* was shown to enhance AeAV replication in *Ae.*
420 *aegypti* cells in this study. Recent studies have demonstrated that *Wolbachia* has no effect on
421 multi-segmented negative-sense RNA viruses; for example, Phasi Charoen-like virus (PCLV)
422 (Family: *Bunyaviridae*) in wMelPop-CLA strain infected Aag2 cells (30), La Crosse virus (Family:
423 *Bunyaviridae*) and vesicular stomatitis virus (Family: *Rhabdoviridae*), which is in the same order as
424 AeAV, in wStri strain in *Ae. albopictus* C710 cell line (83), and the Rift Valley fever virus (RVFV)
425 (Family: *Phenuiviridae*), in *Culex tarsalis* mosquitoes transinfected with a somatic *Wolbachia*
426 (strain wAlbB) had no effect on RVFV infection or dissemination (84), respectively. RVFV and
427 PCLV belong to the *Bunyavirales* order and AeAV belongs to *Mononegavirales*, distinct orders of
428 negative strand RNA viruses. All three viruses have conserved features that may provide insight
429 into how they might be protected from restriction by *Wolbachia*. The genome of all negative-sense
430 ssRNA viruses is both encapsidated within the nucleoprotein (85, 86) and is attached to RNA
431 dependent RNA polymerase within the virion (87). The RNA dependent polymerase complex
432 carries out both transcription of virus genes and replication of the genome.

433 *Wolbachia* has been shown to restrict a number of positive-sense RNA virus species from the
434 *Togaviridae* and *Flaviviridae* families (82). After fusion and entry into the host cell, the genomes of
435 *Togaviridae* and *Flaviviridae* species are released into the cytoplasm and translated directly into
436 polypeptide protein(s). These polypeptide proteins are processed by viral and cellular proteases to
437 generate the mature structural and non-structural proteins which are then used to replicate the
438 genome (88). While the exact mechanism for RNA virus restriction in *Wolbachia*-infected insects
439 has remained elusive, it has been shown that restriction of RNA viruses by *Wolbachia* happens
440 early in infection (89, 90). In the *Ae. albopictus* cell line C710 stably infected with wStri, the
441 polypeptide of ZIKV is not produced as determined by immunoblot at one day post-infection (90).

442 Additionally, *Wolbachia* exploits host innate immunity to establish a symbiotic relationship with *Ae.*
443 *aegypti* (91). Perhaps the combination of protection of the RNA nucleocapsid genome or genome
444 segments when released in the cytoplasm or activity of the RNA-dependent RNA polymerase may
445 aid in evasion of host immune response enhanced by *Wolbachia* or *Wolbachia* effector molecules
446 (92). However, a recent study suggested increases in infection of *Ae. aegypti* mosquitoes by
447 insect-specific flaviviruses when they harbour *Wolbachia* wMel strain (93).

448 The ability of AeAV to modestly reduce DENV-2 genomic RNA in a persistently infected cell line
449 was unexpected. While it has previously been shown that members of the same virus family can
450 provide super exclusion of additional viruses (12, 94), little work has been undertaken to look at
451 cross viral family exclusion effects. Our results showed that less DENV replication occurred in the
452 presence of AeAV, with the difference particularly significant at lower MOI. If this suppressive effect
453 also occurs in mosquitoes, enhancement of AeAV in *Ae. aegypti* mosquitoes infected with
454 *Wolbachia* may be beneficial in terms of DENV suppression.

455 As *Ae. aegypti* is perhaps the most important vector of arboviruses worldwide, further work should
456 be undertaken in understanding and characterising the virome of this mosquito and effects on
457 mosquito life-history traits. Our findings provide new insights into the evolution and genetic
458 diversity of AeAV across a wide geographic range as well as providing valuable insights into the
459 virus features and families restricted by *Wolbachia* in mosquito hosts and its effects on arboviruses
460 they transmit.

461 **Materials and Methods**

462 **Cell lines maintenance and experimental infection with AeAV**

463 *Ae. aegypti* cell line (Aag2) stably infected with *Wolbachia* (denoted Aag2.wMelPop-CLA) as
464 previously described for the C6/36.wMelPop-CLA (35), with its previously generated tetracycline-
465 treated line (66), and both *Ae. albopictus* C6/36 cell line (57) and RML-12 cell lines were
466 maintained in 1:1 Mitsuhashi-Maramorosch and Schneider's insect medium (Invitrogen)
467 supplemented with 10% Fetal Bovine Serum (FBS, Bovogen Biologicals). Aa20 cells established
468 from *Ae. aegypti* larvae (95) were maintained in Leibovitz's L15 medium supplemented with 10%

469 FBS (France – Biowest) and 10% Tryptose phosphate broth at 27°C. African green monkey cells
470 (Vero) were maintained in Opti-MEM I Reduced-Serum Medium supplemented with 2% FBS and
471 10 mL/L Penicillin-Streptomycin (Sigma-Aldrich). Human hepatocellular carcinoma cells (Huh-7)
472 were maintained in Opti-MEM I Reduced-Serum Medium supplemented with 5% FBS and 10 mL/L
473 Penicillin-Streptomycin (Sigma-Aldrich). BSR cells (a clone of Baby Hamster Kidney-21) were
474 maintained in Dulbecco's Modified Eagle Medium (Gibco), 2% FBS and 10 mL/L Penicillin-
475 Streptomycin (Sigma-Aldrich). All mammalian cells were kept at 37°C with 5%CO₂.

476 For experimental infection of cells, 10⁶ cells of *Aedes* or mammalian cells were seeded in a 12-well
477 plate. Subsequently, supernatant from Aag2.ΔMelPop-CLA cells was collected, centrifuged at
478 2150×g for 5 min to remove cells and debris, and used as an AeAV inoculation source. One Aa20
479 cell line was experimentally inoculated with RML-12 cell supernatant and kept as a persistently
480 infected AeAV cell line. Cells were collected at 1, 3 and 5 days post-inoculation for *Aedes* cell lines
481 for RT-qPCR analysis and 1, 3, 5 and 7 days for mammalian cell lines for RT-PCR analysis.

482 ***Aedes anphevirus (AeAV) and dengue virus (DENV-2) interaction assay***

483 The third passage of Aa20 cells persistently infected with AeAV (denoted Aa20_{AeAV}) and Aa20
484 mock were seeded at the density of 3×10⁵ cells in 12-well plates overnight. Cells were then
485 infected with the East Timor (ET-100) DENV-2 strain at a multiplicity of infection (MOI) of 0.1 and
486 1, cells were rocked for an hour at room temperature and supernatant was discarded and replaced
487 with fresh medium. Cells were collected at 0, 1, 3 and 5dpi after infection with mock collected at 5
488 dpi. Cells were subjected to RNA extraction to quantify the DENV-2 genomic RNA levels by RT-
489 qPCR as described below.

490 **Assembly and identification of AeAV strains from RNA-Seq data**

491 For detection of AeAV in previously published RNA-Seq data, we used the assembled RML-12
492 AeAV genome as a BLASTN query for all available *Ae. aegypti* (taxonID: 7159) RNA-Seq data
493 within the Sequence Read Archive (SRA) on NCBI. SRA run files with positive hits of 90-100%
494 identity and an E value <2E-30 were downloaded and converted to fastq using the NCBI SRA
495 toolkit <https://www.ncbi.nlm.nih.gov/sra/docs/toolkitsoft/> for further analysis. FastQC
496 (<https://www.bioinformatics.babraham.ac.uk/projects/fastqc/>) was used for quality checking of fastq

497 files and adapter identification. Fastq files were then imported into CLC Genomics Workbench
498 (10.1.1) and were adapter and quality trimmed (<0.02; equivalent Phred quality score of 17,
499 ambiguous nucleotides: 2).

500 Two strategies were used to assemble strains of AeAV; fastq files from the same source of *Ae.*
501 *aegypti* were pooled and *de novo* assembled using the CLC Genomics Workbench assembly
502 program with automatic bubble and word sizes. This was sufficient to assemble the full coding
503 sequences (CDS) of most strains of AeAV. Table S1 contains *de novo* assembly statistics from
504 each dataset used.

505 If *de novo* assembly did not produce the complete AeAV genome, to complete further sections of
506 the AeAV genome clean reads were mapped to the C6/36.wMelPop-CLA strain of AeAV with
507 stringent alignment criteria (Match score:1 Mismatch cost:2 length fraction 0.89 and similarity
508 fraction 0.89) to exclude false-positive mapping that derives from Endogenous Viral Elements
509 (EVEs). To confirm accuracy of assembly, the largest contigs of consensus mapping were
510 extracted and then used as a reference for re-mapping and manually checked. Final sequences of
511 the virus genomes were obtained through the majority consensus of the mapping assembly and
512 were given Coding Complete (CC) or Standard Draft (SD) genome quality ratings (96).

513 **RNA isolation, strand specific cDNA synthesis and RT-qPCR**

514 Total RNA was extracted from mosquito cells using QIAzol Lysis Reagent (QIAGEN) and treated
515 with Turbo DNase (Thermo Fisher Scientific) as per manufacturer's instructions. RNA quality and
516 quantity were evaluated using a BioTek Epoch Microspot Plate Spectrophotometer. For the
517 production of AeAV genome and anti-genome cDNA, two cDNA reactions were generated using
518 600ng of RNA and SuperScript III Reverse Transcriptase (Thermo Fisher Scientific). The genome
519 cDNA strand was synthesised using a forward primer to AeAV (AeAVGenome-RT 5'-
520 AGACTTCTAAGCCTGCCACA -3'), and the AeAV anti-genome cDNA strand was synthesised
521 using a reverse orientation primer (AeAVAntiGenome-RT 5'- ACACCTTGCCATGTGCTCAG -3').
522 *Aedes* Ribosomal protein subunit 17 (RPS17) primers (*Ae. aegypti*: AeRPS17-qR 5'-
523 GGACACTTCGGGCACGTAGT-3' and *Ae. albopictus* AaIRPS17q-R 5'-
524 ACGTAGTTGTCTCTCTGCGCTC -3') were used for reference gene cDNA synthesis. Following

525 RT, qPCR with AeAV primers (AeAV-qF 5'-GACAATCGCATTGGCTGCAT-3' and AeAV-qR 5'-
526 CCCGAGACAATCGGCTTCTT - 3') as well as primer pairs for the RPS17 genes (*Ae. aegypti*:
527 AeRPS17-qF 5'- CACTCCGAGGTCCGTGGTAT -3' and *Ae. albopictus*: AalRPS17-qF 5'-
528 CGCTGGTTTCGTGACACATC -3') were undertaken. RPS17 was used for normalizing data as
529 described previously in *Ae. aegypti* cells (97).

530 For quantitation of DENV-2 genome copies in Aa20 cells, two SuperScript III reverse transcription
531 (Thermo Fisher Scientific) reactions with 1000ng of RNA were prepared. For DENV-2 genome
532 copies reaction, the reverse primer (DENV2-qR 5'- CAAGGCTAACGCATCAGTCA -3') and in a
533 separate cDNA synthesis reaction the *Ae. aegypti* RPS17 primers as described above.
534 Subsequently, qPCR for DENV-2 was carried out using the DENV-2 primer pair (DENV2-qF 5'-
535 GGTATGGTGGGCGCTACTA -3' and DENV2-qR), and RPS17 was used as a normalising control
536 as also described above.

537 Each time-point for experimental infection was run with three biological replicates and two technical
538 replicates. Platinum SYBR Green Mix (Invitrogen) was used for qPCR with 20ng of RT products in
539 a Rotor-Gene thermal cycler (QIAGEN) as described above. The relative abundance of AeAV RNA
540 and DENV-2 to the host reference gene was determined by qGENE software using the $\Delta\Delta C_t$
541 method and analyzed using GraphPad Prism.

542 To test for the replication of AeAV in mammalian cells, 1000ng of total RNA extracted from the
543 cells was extracted and used for first stand synthesis with SuperScript III reverse transcriptase with
544 the AeAVGenome-RT primer. qPCR was subsequently carried out using AeAVGenome-RT primer
545 and the qPCR primer AeAVqR2 5'-ATGAAAGTATGGATACACACCGCG-3'. Products were then
546 visualised on a 1% agarose gel.

547 **Virus genome annotation**

548 Potential ORFs of AeAV were analysed using NCBI Open Reading Frame Finder
549 (<https://www.ncbi.nlm.nih.gov/orffinder/>) with a minimal ORF length of 150. ORFs were cross
550 referenced with mapping from Poly(A) enriched transcriptomes (Fig. S1) to reduce false positive
551 identification of ORFs. For determination of putative domains in AeAV, ORFs were translated and
552 searched against the Conserved Domain Search Service (CD Search)

553 (<https://www.ncbi.nlm.nih.gov/Structure/cdd/wrpsb.cgi>). For protein homology detection, we used
554 the HHPred webserver on translated AeAV ORFs (98).

555 To best discriminate N-terminus transmembrane domains from signal peptides, we used the
556 consensus TOPCONS webserver (99). Glycosylation sites were predicted by the NetNGlyc 1.0/
557 NetOGlyc 4.0 Server (<http://www.cbs.dtu.dk/services/>).

558 **Phylogenetic analysis**

559 For placement of AeAV within the order *Mononegavirales*, ClustalW was used on CLC Genomics
560 Workbench to align amino acid sequences of 30 L proteins of the most closely related
561 *Mononegavirales* species as determined by BLASTp of the NCBI non-redundant database. A
562 Maximum likelihood phylogeny (PhyML) was constructed using the Whelan and Goldman (WAG)
563 amino acid substitution model with 1000 bootstraps. Accession numbers and associated hosts
564 used to produce the phylogenetic tree are available in Table S1.

565 To determine relatedness between different strains of AeAV, genomes that were coding complete
566 and greater than 30x coverage were trimmed of 3'UTR and 5'UTR regions and aligned using the
567 ClustalW algorithm on CLC Genomics Workbench. A Maximum likelihood phylogeny (PhyML) was
568 constructed. A Hierarchical likelihood ratio test (hLRT) with a confidence level of 0.01 suggested
569 that the General Time Reversible (GTR) +G (Rate variation 4 categories) and +T (topology
570 variation) nucleotide substitution model was the most appropriate. 1000 bootstrap replicates were
571 performed with 95% bootstrap branching support cut-off.

572 **Statistical analysis**

573 Statistical analysis Unpaired t-test was used to compare differences between two individual
574 groups, while One-way ANOVA with Tukey's post-hoc test was carried out to compare differences
575 between more than two groups. Data that did not pass the normality test were re-analysed by the
576 non-parametric Wilcoxon test indicated in their relevant figure legends.

577 **Accession numbers**

578 All complete virus genome sequences generated in this study have been deposited in Genbank
579 under the accession numbers (MH037149-MH037164). The incomplete Cayenne and St Georges

580 French Guiana AeAV contigs have been placed in supplementary File S1 alongside
581 Aag2.wMelPop-CLA and C6/36.wMel-CLA strains.

582 Acknowledgements

583 This project was funded by the Australian Research Council grant (ARC, DP150101782) to SA and
584 University of Queensland scholarship to RP. For the supply of the DENV-2 (ET-100) strain, we
585 thank Dr Daniel Watterson and Professor Paul Young from the University of Queensland. We
586 thank Dr Daniel Watterson and Dr Jody Hobson-Peters for providing Huh-7 and BSR cells,
587 respectively. The authors would like to thank the technical assistance of Dr Sultan Asad, Dr
588 Kayvan Etebari and Hugo Perdomo Contreras, as well as current and former members of the
589 Asgari lab for their fruitful conversations.

590 References

- 591 1. **Shriram AN, Sivan A, Sugunan AP.** 2017. Spatial distribution of *Aedes aegypti*
592 and *Aedes albopictus* in relation to geo-ecological features in South Andaman,
593 Andaman and Nicobar Islands, India. *Bull Entomol Res* **3**:166-174.
- 594 2. **Bhatt S, Gething PW, Brady OJ, Messina JP, Farlow AW, Moyes CL, Drake JM,**
595 **Brownstein JS, Hoen AG, Sankoh O, Myers MF, George DB, Jaenisch T, Wint**
596 **GR, Simmons CP, Scott TW, Farrar JJ, Hay SI.** 2013. The global distribution and
597 burden of dengue. *Nature* **496**:504-507.
- 598 3. **ECDC.** 2015. Rapid risk assessment: Zika virus epidemic in the Americas: potential
599 association with microcephaly and Guillain-Barré syndrome. European Centre for
600 Disease Prevention and Control S,
601 [https://ecdc.europa.eu/sites/portal/files/media/en/publications/Publications/zika-](https://ecdc.europa.eu/sites/portal/files/media/en/publications/Publications/zika-virus-americas-association-with-microcephaly-rapid-risk-assessment.pdf)
602 [virus-americas-association-with-microcephaly-rapid-risk-assessment.pdf](https://ecdc.europa.eu/sites/portal/files/media/en/publications/Publications/zika-virus-americas-association-with-microcephaly-rapid-risk-assessment.pdf).
- 603 4. **Tabachnick WJ.** 2013. Nature, nurture and evolution of intra-species variation in
604 mosquito arbovirus transmission competence. *Int J Environ Res Public Health*
605 **10**:249-277.
- 606 5. **Weiss B, Aksoy S.** 2011. Microbiome influences on insect host vector competence.
607 *Trends Parasitol* **27**:514-522.
- 608 6. **Beerntsen BT, James AA, Christensen BM.** 2000. Genetics of mosquito vector
609 competence. *Microbiol Mol Biol Rev* **64**:115-137.
- 610 7. **Hall RA, Bielefeldt-Ohmann H, McLean BJ, O'Brien CA, Colmant AM, Piyasena**
611 **TB, Harrison JJ, Newton ND, Barnard RT, Prow NA, Deerrain JM, Mah MG,**
612 **Hobson-Peters J.** 2016. Commensal viruses, transmission, and interaction with
613 arboviral pathogens. *Evol Bioinform Online* **12**:35-44.
- 614 8. **Blitvich BJ, Firth AE.** 2015. Insect-specific flaviviruses: a systematic review of their
615 discovery, host range, mode of transmission, superinfection exclusion potential and
616 genomic organization. *Viruses* **7**:1927-1959.
- 617 9. **van Cleef KW, van Mierlo JT, Miesen P, Overheul GJ, Fros JJ, Schuster S,**
618 **Marklewitz M, Pijlman GP, Junglen S, van Rij RP.** 2014. Mosquito and
619 *Drosophila* entomobirnaviruses suppress dsRNA- and siRNA-induced RNAi.
620 *Nucleic Acids Res* **42**:8732-8744.

- 621 10. **Zhang G, Asad S, Khromykh AA, Asgari S.** 2017. Cell fusing agent virus and
622 dengue virus mutually interact in *Aedes aegypti* cell lines. *Sci Rep* **7**:6935.
- 623 11. **Hobson-Peters J, Yam AW, Lu JW, Setoh YX, May FJ, Kurucz N, Walsh S,**
624 **Prow NA, Davis SS, Weir R, Melville L, Hunt N, Webb RI, Blitvich BJ, Whelan**
625 **P, Hall RA.** 2013. A new insect-specific flavivirus from northern Australia
626 suppresses replication of West Nile virus and Murray Valley encephalitis virus in co-
627 infected mosquito cells. *PLoS One* **8**:e56534.
- 628 12. **Hall-Mendelin S, McLean BJ, Bielefeldt-Ohmann H, Hobson-Peters J, Hall RA,**
629 **van den Hurk AF.** 2016. The insect-specific Palm Creek virus modulates West Nile
630 virus infection in and transmission by Australian mosquitoes. *Parasit Vectors* **9**:414.
- 631 13. **Schultz MJ, Frydman HM, Connor JH.** 2018. Dual Insect specific virus infection
632 limits Arbovirus replication in *Aedes* mosquito cells. *Virology* **518**:406-413.
- 633 14. **Chandler JA, Liu RM, Bennett SN.** 2015. RNA shotgun metagenomic sequencing
634 of northern California (USA) mosquitoes uncovers viruses, bacteria, and fungi.
635 *Front Microbiol* **6**:185.
- 636 15. **Fauver JR, Grubaugh ND, Krajacich BJ, Weger-Lucarelli J, Lakin SM, Fakoli**
637 **LS, 3rd, Bolay FK, Diclaro JW, 2nd, Dabire KR, Foy BD, Brackney DE, Ebel**
638 **GD, Stenglein MD.** 2016. West African *Anopheles gambiae* mosquitoes harbor a
639 taxonomically diverse virome including new insect-specific flaviviruses,
640 mononegaviruses, and totiviruses. *Virology* **498**:288-299.
- 641 16. **Bolling BG, Vasilakis N, Guzman H, Widen SG, Wood TG, Popov VL,**
642 **Thangamani S, Tesh RB.** 2015. Insect-specific viruses detected in laboratory
643 mosquito colonies and their potential implications for experiments evaluating
644 arbovirus vector competence. *Am J Trop Med Hyg* **92**:422-428.
- 645 17. **Cook S, Bennett SN, Holmes EC, De Chesse R, Moureau G, de Lamballerie X.**
646 2006. Isolation of a new strain of the flavivirus cell fusing agent virus in a natural
647 mosquito population from Puerto Rico. *J Gen Virol* **87**:735-748.
- 648 18. **Chandler JA, Thongsripong P, Green A, Kittayapong P, Wilcox BA, Schroth**
649 **GP, Kapan DD, Bennett SN.** 2014. Metagenomic shotgun sequencing of a
650 Bunyavirus in wild-caught *Aedes aegypti* from Thailand informs the evolutionary
651 and genomic history of the Phleboviruses. *Virology* **464-465**:312-319.
- 652 19. **Vasilakis N, Forrester NL, Palacios G, Nasar F, Savji N, Rossi SL, Guzman H,**
653 **Wood TG, Popov V, Gorchakov R, Gonzalez AV, Haddow AD, Watts DM, da**
654 **Rosa AP, Weaver SC, Lipkin WI, Tesh RB.** 2013. Negevirus: a proposed new
655 taxon of insect-specific viruses with wide geographic distribution. *J Virol* **87**:2475-
656 2488.
- 657 20. **Kittayapong P, Baisley KJ, O'Neill SL.** 1999. A mosquito densovirus infecting
658 *Aedes aegypti* and *Aedes albopictus* from Thailand. *Am J Trop Med Hyg* **61**:612-
659 617.
- 660 21. **Aguiar ER, Olmo RP, Paro S, Ferreira FV, de Faria IJ, Todjro YM, Lobo FP,**
661 **Kroon EG, Meignin C, Gatherer D, Imler JL, Marques JT.** 2015. Sequence-
662 independent characterization of viruses based on the pattern of viral small RNAs
663 produced by the host. *Nucleic Acids Res* **43**:6191-6206.
- 664 22. **Zakrzewski M, Rasic G, Darbro J, Krause L, Poo YS, Filipovic I, Parry R,**
665 **Asgari S, Devine G, Suhrbier A.** 2018. Mapping the virome in wild-caught *Aedes*
666 *aegypti* from Cairns and Bangkok. *Sci Rep* **16**:4690.
- 667 23. **Amarasinghe GK, Bao Y, Basler CF, Bavari S, Beer M, Bejerman N, Blasdel**
668 **KR, Bochnowski A, Briese T, Bukreyev A, Calisher CH, Chandran K, Collins**
669 **PL, Dietzgen RG, Dolnik O, Durrwald R, Dye JM, Easton AJ, Ebihara H, Fang**
670 **Q, Formenty P, Fouchier RAM, Ghedin E, Harding RM, Hewson R, Higgins CM,**
671 **Hong J, Horie M, James AP, Jiang D, Kobinger GP, Kondo H, Kurath G, Lamb**
672 **RA, Lee B, Leroy EM, Li M, Maisner A, Muhlberger E, Netesov SV, Nowotny N,**

- 673 **Patterson JL, Payne SL, Paweska JT, Pearson MN, Randall RE, Revill PA,**
674 **Rima BK, Rota P, Rubbenstroth D, et al.** 2017. Taxonomy of the order
675 Mononegavirales: update 2017. *Arch Virol* **162**:2493-2504.
- 676 24. **Li CX, Shi M, Tian JH, Lin XD, Kang YJ, Chen LJ, Qin XC, Xu J, Holmes EC,**
677 **Zhang YZ.** 2015. Unprecedented genomic diversity of RNA viruses in arthropods
678 reveals the ancestry of negative-sense RNA viruses. *eLife* **4**:e05378.
- 679 25. **Shi M, Neville P, Nicholson J, Eden JS, Imrie A, Holmes EC.** 2017. High-
680 resolution metatranscriptomics reveals the ecological dynamics of mosquito-
681 associated RNA viruses in Western Australia. *J Virol* **91**:e00680-00617.
- 682 26. **Hedges LM, Brownlie JC, O'Neill SL, Johnson KN.** 2008. *Wolbachia* and virus
683 protection in insects. *Science* **322**:702.
- 684 27. **Teixeira L, Ferreira A, Ashburner M.** 2008. The bacterial symbiont *Wolbachia*
685 induces resistance to RNA viral infections in *Drosophila melanogaster*. *PLoS Biol*
686 **6**:e2.
- 687 28. **Moreira LA, Iturbe-Ormaetxe I, Jeffery JA, Lu G, Pyke AT, Hedges LM, Rocha**
688 **BC, Hall-Mendelin S, Day A, Riegler M, Hugo LE, Johnson KN, Kay BH,**
689 **McGraw EA, van den Hurk AF, Ryan PA, O'Neill SL.** 2009. A *Wolbachia*
690 symbiont in *Aedes aegypti* limits infection with dengue, Chikungunya, and
691 *Plasmodium*. *Cell* **139**:1268-1278.
- 692 29. **Zhang G, Etebari K, Asgari S.** 2016. *Wolbachia* suppresses cell fusing agent virus
693 in mosquito cells. *J Gen Virol* **97**:3427-3432.
- 694 30. **Schnettler E, Sreenu VB, Mottram T, McFarlane M.** 2016. *Wolbachia* restricts
695 insect-specific flavivirus infection in *Aedes aegypti* cells. *J Gen Virol* **97**:3024-3029.
- 696 31. **Sabin LR, Zheng Q, Thekkat P, Yang J, Hannon GJ, Gregory BD, Tudor M,**
697 **Cherry S.** 2013. Dicer-2 processes diverse viral RNA species. *PLoS One*
698 **8**:e55458.
- 699 32. **Sanchez-Vargas I, Scott JC, Poole-Smith BK, Franz AW, Barbosa-Solomieu V,**
700 **Wilusz J, Olson KE, Blair CD.** 2009. Dengue virus type 2 infections of *Aedes*
701 *aegypti* are modulated by the mosquito's RNA interference pathway. *PLoS Pathog*
702 **5**:e1000299.
- 703 33. **Wu Q, Luo Y, Lu R, Lau N, Lai EC, Li WX, Ding SW.** 2010. Virus discovery by
704 deep sequencing and assembly of virus-derived small silencing RNAs. *Proc Natl*
705 *Acad Sci U S A* **107**:1606-1611.
- 706 34. **Mayoral JG, Etebari K, Hussain M, Khromykh AA, Asgari S.** 2014. *Wolbachia*
707 infection modifies the profile, shuttling and structure of microRNAs in a mosquito
708 cell line. *PLoS One* **9**:e96107.
- 709 35. **Frentiu FD, Robinson J, Young PR, McGraw EA, O'Neill SA.** 2010. *Wolbachia*-
710 mediated resistance to Dengue virus infection and death at the cellular level. *PLoS*
711 *One* **5**:e13398.
- 712 36. **McMeniman CJ, Lane AM, Fong AW, Voronin DA, Iturbe-Ormaetxe I, Yamada**
713 **R, McGraw EA, O'Neill SL.** 2008. Host adaptation of a *Wolbachia* strain after long-
714 term serial passage in mosquito cell lines. *Appl Environ Microbiol* **74**:6963-6969.
- 715 37. **Darby AC, Gill AC, Armstrong SD, Hartley CS, Xia D, Wastling JM, Makepeace**
716 **BL.** 2014. Integrated transcriptomic and proteomic analysis of the global response
717 of *Wolbachia* to doxycycline-induced stress. *ISME J* **8**:925-937.
- 718 38. **Woolfit M, Algama M, Keith JM, McGraw EA, Popovici J.** 2015. Discovery of
719 putative small non-coding RNAs from the obligate intracellular bacterium *Wolbachia*
720 *pipientis*. *PLoS One* **10**:e0118595.
- 721 39. **Green TJ, Cox R, Tsao J, Rowse M, Qiu S, Luo M.** 2014. Common mechanism
722 for RNA encapsidation by negative-strand RNA viruses. *J Virol* **88**:3766-3775.

- 723 40. **Baron OL, Ursic-Bedoya RJ, Lowenberger CA, Ocampo CB.** 2010. Differential
724 gene expression from midguts of refractory and susceptible lines of the mosquito,
725 *Aedes aegypti*, infected with Dengue-2 virus. *J Insect Sci* **10**:41.
- 726 41. **Iverson LE, Rose JK.** 1981. Localized attenuation and discontinuous synthesis
727 during vesicular stomatitis virus transcription. *Cell* **23**:477-484.
- 728 42. **Ferron F, Longhi S, Henrissat B, Canard B.** 2002. Viral RNA-polymerases -- a
729 predicted 2'-O-ribose methyltransferase domain shared by all Mononegavirales.
730 *Trends Biochem Sci* **27**:222-224.
- 731 43. **Bailey TL, Boden M, Buske FA, Frith M, Grant CE, Clementi L, Ren J, Li WW,
732 Noble WS.** 2009. MEME SUITE: tools for motif discovery and searching. *Nucleic
733 Acids Res* **37**:W202-208.
- 734 44. **Lorenz R, Bernhart SH, Honer Zu Siederdisen C, Tafer H, Flamm C, Stadler
735 PF, Hofacker IL.** 2011. ViennaRNA Package 2.0. *Algorithms Mol Biol* **6**:26.
- 736 45. **Miller WA, Giedroc D.** 2010. Ribosomal frameshifting in decoding plant viral RNAs,
737 p 193–220. *In* Atkins JF, Gesteland RF (ed), *Recoding: expansion of decoding rules
738 enriches gene expression*. Springer, New York.
- 739 46. **Walker PJ, Firth C, Widen SG, Blasdel KR, Guzman H, Wood TG, Paradkar
740 PN, Holmes EC, Tesh RB, Vasilakis N.** 2015. Evolution of genome size and
741 complexity in the *Rhabdoviridae*. *PLoS Pathog* **11**:e1004664.
- 742 47. **Lewis SH, Quarles KA, Yang Y, Tanguy M, Frezal L, Smith SA, Sharma PP,
743 Cordaux R, Gilbert C, Giraud I, Collins DH, Zamore PD, Miska EA, Sarkies P,
744 Jiggins FM.** 2018. Pan-arthropod analysis reveals somatic piRNAs as an ancestral
745 defence against transposable elements. *Nat Ecol Evol* **2**:174-181.
- 746 48. **Suzuki Y, Frangeul L, Dickson LB, Blanc H, Verdier Y, Vinh J, Lambrechts L,
747 Saleh MC.** 2017. Uncovering the repertoire of endogenous flaviviral elements in
748 *Aedes* mosquito genomes. *J Virol* **91**.
- 749 49. **McBride CS, Baier F, Omondi AB, Spitzer SA, Lutomiah J, Sang R, Ignell R,
750 Vosshall LB.** 2014. Evolution of mosquito preference for humans linked to an
751 odorant receptor. *Nature* **515**:222-227.
- 752 50. **Bonizzoni M, Dunn WA, Campbell CL, Olson KE, Marinotti O, James AA.** 2012.
753 Complex modulation of the *Aedes aegypti* transcriptome in response to dengue
754 virus infection. *PLoS One* **7**:e50512.
- 755 51. **Bonizzoni M, Dunn WA, Campbell CL, Olson KE, Marinotti O, James AA.** 2012.
756 Strain variation in the transcriptome of the dengue fever vector, *Aedes aegypti*. *G3*
757 **2**:103-114.
- 758 52. **Faucon F, Gaude T, Dusfour I, Navratil V, Corbel V, Juntarajumnong W, Girod
759 R, Poupardin R, Boyer F, Reynaud S, David JP.** 2017. In the hunt for genomic
760 markers of metabolic resistance to pyrethroids in the mosquito *Aedes aegypti*: An
761 integrated next-generation sequencing approach. *PLoS Negl Trop Dis*
762 **11**:e0005526.
- 763 53. **Alfonso-Parra C, Ahmed-Braimah YH, Degner EC, Avila FW, Villarreal SM,
764 Pleiss JA, Wolfner MF, Harrington LC.** 2016. Mating-induced transcriptome
765 changes in the reproductive tract of female *Aedes aegypti*. *PLoS Negl Trop Dis*
766 **10**:e0004451.
- 767 54. **Sutton ER, Yu Y, Shimeld SM, White-Cooper H, Alphey AL.** 2016. Identification
768 of genes for engineering the male germline of *Aedes aegypti* and *Ceratitis capitata*.
769 *BMC Genomics* **17**:948.
- 770 55. **David JP, Faucon F, Chandor-Proust A, Poupardin R, Riaz MA, Bonin A,
771 Navratil V, Reynaud S.** 2014. Comparative analysis of response to selection with
772 three insecticides in the dengue mosquito *Aedes aegypti* using mRNA sequencing.
773 *BMC Genomics* **15**:174.

- 774 56. **Metsky HC, Matranga CB, Wohl S, Schaffner SF, Freije CA, Winnicki SM, West**
775 **K, Qu J, Baniecki ML, Gladden-Young A, Lin AE, Tomkins-Tinch CH, Ye SH,**
776 **Park DJ, Luo CY, Barnes KG, Shah RR, Chak B, Barbosa-Lima G, Delatorre E,**
777 **Vieira YR, Paul LM, Tan AL, Barcellona CM, Porcelli MC, Vasquez C, Cannons**
778 **AC, Cone MR, Hogan KN, Kopp EW, Anzinger JJ, Garcia KF, Parham LA,**
779 **Ramirez RMG, Montoya MCM, Rojas DP, Brown CM, Hennigan S, Sabina B,**
780 **Scotland S, Gangavarapu K, Grubaugh ND, Oliveira G, Robles-Sikisaka R,**
781 **Rambaut A, Gehrke L, Smole S, Halloran ME, Villar L, Mattar S, et al. 2017.**
782 **Zika virus evolution and spread in the Americas. *Nature* 546:411-415.**
- 783 57. **Singh K. 1967. Cell cultures derived from larvae of *Aedes albopictus* (Skuse) and**
784 ***Aedes aegypti* (L.). *Curr Sci* 36:506-508.**
- 785 58. **Powell JR, Tabachnick WJ. 2013. History of domestication and spread of *Aedes***
786 ***aegypti*--a review. *Mem Inst Oswaldo Cruz* 108 Suppl 1:11-17.**
- 787 59. **Brown JE, Evans BR, Zheng W, Obas V, Barrera-Martinez L, Egizi A, Zhao H,**
788 **Caccone A, Powell JR. 2014. Human impacts have shaped historical and recent**
789 **evolution in *Aedes aegypti*, the dengue and yellow fever mosquito. *Evolution***
790 **68:514-525.**
- 791 60. **Gloria-Soria A, Ayala D, Bheecarry A, Calderon-Arguedas O, Chadee DD,**
792 **Chiappero M, Coetzee M, Elahee KB, Fernandez-Salas I, Kamal HA, Kamgang**
793 **B, Khater El, Kramer LD, Kramer V, Lopez-Solis A, Lutomiah J, Martins A, Jr.,**
794 **Mieli MV, Paupy C, Ponlawat A, Rahola N, Rasheed SB, Richardson JB,**
795 **Saleh AA, Sanchez-Casas RM, Seixas G, Sousa CA, Tabachnick WJ, Troyo A,**
796 **Powell JR. 2016. Global genetic diversity of *Aedes aegypti*. *Mol Ecol* 25:5377-**
797 **5395.**
- 798 61. **Suzuki Y, Frangeul L, Dickson LB, Blanc H, Verdier Y, Vinh J, Lambrechts L,**
799 **Saleh MC. 2017. Uncovering the repertoire of endogenous flaviviral elements in**
800 ***Aedes* mosquito genomes. *J Virol* 91:e00571-00517.**
- 801 62. **Whitfield ZJ, Dolan PT, Kunitomi M, Tassetto M, Seetin MG, Oh S, Heiner C,**
802 **Paxinos E, Andino R. 2017. The diversity, structure, and function of heritable**
803 **adaptive immunity sequences in the *Aedes aegypti* genome. *Curr Biol* 27:3511-**
804 **3519 e3517.**
- 805 63. **Vodovar N, Bronkhorst A, van Cleef K, Miesen P, Blanc H, van Rij R, MC S.**
806 **2012. Arbovirus-derived piRNAs exhibit a ping-pong signature in mosquito cells.**
807 ***PLoS One* 7:e30861.**
- 808 64. **Brackney DE, Scott JC, Sagawa F, Woodward JE, Miller NA, Schilkey FD,**
809 **Mudge J, Wilusz J, Olson KE, Blair CD, Ebel GD. 2010. C6/36 *Aedes albopictus***
810 **cells have a dysfunctional antiviral RNA interference response. *PLoS Neglect Trop***
811 **Dis 4:e856.**
- 812 65. **Léger P, Lara E, Jagla B, Sismeiro O, Mansuroglu Z, Coppée J, Bonnefoy E,**
813 **Bouloy M. 2013. Dicer-2- and Piwi-mediated RNA interference in Rift Valley fever**
814 **virus-infected mosquito cells. *J Virol* 87:1631-1648.**
- 815 66. **Asad S, Parry R, Asgari S. 2017. Upregulation of *Aedes aegypti* *Vago1* by**
816 ***Wolbachia* and its effect on dengue virus replication. *Insect Biochem Mol Biol***
817 **92:45-52.**
- 818 67. **Miesen P, Joosten J, van Rij RP. 2016. PIWIs go viral: Arbovirus-derived piRNAs**
819 **in vector mosquitoes. *PLoS Pathog* 12:e1006017.**
- 820 68. **Di Giallonardo F, Audsley MD, Shi M, Young PR, McGraw EA, Holmes EC.**
821 **2018. Complete genome of *Aedes aegypti* anphevirus in the Aag2 mosquito cell**
822 **line. *J Gen Virol* doi: 10.1099/jgv.0.001079.**
- 823 69. **Lee M, Etebari K, Hall-Mendelin S, van den Hurk AF, Hobson-Peters J,**
824 **Vatipally S, Schnettler E, Hall R, Asgari S. 2017. Understanding the role of**

- 825 microRNAs in the interaction of *Aedes aegypti* mosquitoes with an insect-specific
826 flavivirus. *J Gen Virol* **98**:1892-1903.
- 827 70. **Etebari K, Osei-Amo S, Blomberg SP, Asgari S.** 2015. Dengue virus infection
828 alters post-transcriptional modification of microRNAs in the mosquito vector *Aedes*
829 *aegypti*. *Sci Rep* **5**:15968.
- 830 71. **Kuno G.** 1983. Cultivation of mosquito cell lines in serum-free media and their
831 effects on dengue virus replication. *In Vitro* **19**:707-713.
- 832 72. **O'Neill SL, Kittayapong P, Braig HR, Andreadis TG, Gonzalez JP, Tesh RB.**
833 1995. Insect densoviruses may be widespread in mosquito cell lines. *J Gen Virol* **76**
834 **(Pt 8)**:2067-2074.
- 835 73. **Juliano SA, Lounibos LP, O'Meara GF.** 2004. A field test for competitive effects of
836 *Aedes albopictus* on *A. aegypti* in South Florida: differences between sites of
837 coexistence and exclusion? *Oecologia* **139**:583-593.
- 838 74. **Blair C, Olson K.** 2015. The role of RNA interference (RNAi) in arbovirus-vector
839 interactions. *Viruses* **7**:820-843.
- 840 75. **Hussain M, Etebari K, Asgari S.** 2016. Functions of small RNAs in mosquitoes.
841 *Adv Insect Physiol* **51**:189-222.
- 842 76. **Schnettler E, Donald CL, Human S, Watson M, Siu RW, McFarlane M,**
843 **Fazakerley JK, Kohl A, Fragkoudis R.** 2013. Knockdown of piRNA pathway
844 proteins results in enhanced Semliki Forest virus production in mosquito cells. *J*
845 *Gen Virol* **94**:1680-1689.
- 846 77. **Dietrich I, Shi X, McFarlane M, Watson M, Blomstrom AL, Skelton JK, Kohl A,**
847 **Elliott RM, Schnettler E.** 2017. The antiviral RNAi response in vector and non-
848 vector cells against Orthobunyaviruses. *PLoS Negl Trop Dis* **11**:e0005272.
- 849 78. **Hess AM, Prasad AN, Ptitsyn A, Ebel GD, Olson EN, Barbacioru C, Monighetti**
850 **C, Campbell CL.** 2011. Small RNA profiling of Dengue virus-mosquito interactions
851 implicates the PIWI RNA pathway in anti-viral defense. *BMC Microbiol* **11**:45.
- 852 79. **Varjak M, Donald CL, Mottram TJ, Sreenu VB, Merits A, Maringer K, Schnettler**
853 **E, Kohl A.** 2017. Characterization of the Zika virus induced small RNA response in
854 *Aedes aegypti* cells. *PLoS Negl Trop Dis* **11**:e0006010.
- 855 80. **Saldaña MA, Etebari K, Hart CE, Widen SG, Wood TG, Thangamani S, Asgari**
856 **S, Hughes GL.** 2017. Zika virus alters the microRNA expression profile and elicits
857 an RNAi response in *Aedes aegypti* mosquitoes. *PLoS Neg Trop Dis* **11**:e0005760.
- 858 81. **Lee M, Etebari K, Hall-Mendelin S, van den Hurk AF, Hobson-Peters J,**
859 **Vatipally S, Schnettler E, Hall R, Asgari S.** 2017. Understanding the role of
860 microRNAs in the interaction of *Aedes aegypti* mosquitoes with an insect-specific
861 flavivirus. *J Gen Virol* **98**:892-1903.
- 862 82. **Johnson KN.** 2015. The impact of *Wolbachia* on virus infection in mosquitoes.
863 *Viruses* **7**:5705-5717.
- 864 83. **Schultz MJ, Tan AL, Gray CN, Isern S, Michael SF, Frydman HM, Connor JH.**
865 2018. *Wolbachia* wStri blocks Zika virus growth at two independent stages of viral
866 replication. *MBio* **9**:e00738-00718.
- 867 84. **Dodson BL, Andrews ES, Turell MJ, Rasgon JL.** 2017. *Wolbachia* effects on Rift
868 Valley fever virus infection in *Culex tarsalis* mosquitoes. *PLoS Negl Trop Dis*
869 **11**:e0006050.
- 870 85. **Hornak KE, Lanchy JM, Lodmell JS.** 2016. RNA encapsidation and packaging in
871 the phleboviruses. *Viruses* **8**:E194.
- 872 86. **Raymond DD, Piper ME, Gerrard SR, Skinotis G, Smith JL.** 2012.
873 Phleboviruses encapsidate their genomes by sequestering RNA bases. *Proc Natl*
874 *Acad Sci U S A* **109**:19208-19213.
- 875 87. **Choi KH.** 2012. Viral polymerases. *Adv Exp Med Biol* **726**:267-304.

- 876 88. **Harak C, Lohmann V.** 2015. Ultrastructure of the replication sites of positive-strand
877 RNA viruses. *Virology* **479-480**:418-433.
- 878 89. **Rainey SM, Martinez J, McFarlane M, Juneja P, Sarkies P, Lulla A, Schnettler**
879 **E, Varjak M, Merits A, Miska EA, Jiggins FM, Kohl A.** 2016. *Wolbachia* blocks
880 viral genome replication early in infection without a transcriptional response by the
881 endosymbiont or host small RNA pathways. *PLoS Pathog* **12**:e1005536.
- 882 90. **Schultz MJ, Isern S, Michael SF, Corley RB, Connor JH, Frydman HM.** 2017.
883 Variable inhibition of Zika virus replication by different *Wolbachia* strains in
884 mosquito cell cultures. *J Virol* **91**:e00339-00317.
- 885 91. **Pan X, Pike A, Joshi D, Bian G, McFadden MJ, Lu P, Liang X, Zhang F, Raikhel**
886 **AS, Xi Z.** 2018. The bacterium *Wolbachia* exploits host innate immunity to establish
887 a symbiotic relationship with the dengue vector mosquito *Aedes aegypti*. *ISME J*
888 **12**:277-288.
- 889 92. **Rice DW, Sheehan KB, Newton ILG.** 2017. Large-scale identification of *Wolbachia*
890 *pipientis* effectors. *Genome Biol Evol* **9**:1925-1937.
- 891 93. **Amuzu HE, Tsyganov K, Koh C, Herbert RI, Powell DR, McGraw EA.** 2018.
892 *Wolbachia* enhances insect-specific flavivirus infection in *Aedes aegypti*
893 mosquitoes. *J Gen Virol* DOI: [10.1002/ece3.4066](https://doi.org/10.1002/ece3.4066).
- 894 94. **Karpf AR, Lenches E, Strauss EG, Strauss JH, Brown DT.** 1997. Superinfection
895 exclusion of alphaviruses in three mosquito cell lines persistently infected with
896 Sindbis virus. *J Virol* **71**:7119-7123.
- 897 95. **Pudney M, Varma M, Leake C.** 1979. Establishment of cell lines from larvae of
898 culicine (*Aedes* species) and anopheline mosquitoes. *TCA Manual* **5**:997-1002.
- 899 96. **Ladner JT, Beitzel B, Chain PS, Davenport MG, Donaldson EF, Frieman M,**
900 **Kugelman JR, Kuhn JH, O'Rear J, Sabeti PC, Wentworth DE, Wiley MR, Yu GY,**
901 **Threat Characterization C, Sozhamannan S, Bradburne C, Palacios G.** 2014.
902 Standards for sequencing viral genomes in the era of high-throughput sequencing.
903 *MBio* **5**:e01360-01314.
- 904 97. **Hussain M, Frentiu FD, Moreira LA, O'Neill SL, Asgari S.** 2011. *Wolbachia* uses
905 host microRNAs to manipulate host gene expression and facilitate colonization of
906 the dengue vector *Aedes aegypti*. *Proc Natl Acad Sci U S A* **108**:9250-9255.
- 907 98. **Zimmermann L, Stephens A, Nam SZ, Rau D, Kubler J, Lozajic M, Gabler F,**
908 **Soding J, Lupas AN, Alva V.** 2017. A completely reimplemented MPI
909 bioinformatics toolkit with a new HHpred server at its core. *J Mol Biol* doi:
910 [10.1016/j.jmb.2017.12.007](https://doi.org/10.1016/j.jmb.2017.12.007).
- 911 99. **Tsirigos KD, Peters C, Shu N, Kall L, Elofsson A.** 2015. The TOPCONS web
912 server for consensus prediction of membrane protein topology and signal peptides.
913 *Nucleic Acids Res* **43**:W401-407.

914 **Figure legends:**

915 **Figure 1. Presence of Aedes anphevirus (AeAV) in insect cell lines, and genome**
916 **organisation and phylogeny of the virus. A)** RT-PCR analysis of *Aedes* cell lines Aag2,
917 Aag2.wMelPop-CLA (Pop), wMelPop-CLA.Tet (Pop-T), Aa20, RML-12, and C6/36 for the
918 presence of AeAV. RPS17 was used as a loading control. **B)** Genome organisation of the
919 Cali, Colombia AeAV genome strain and subgenomic gene transcription profile.
920 Transmembrane domains (TMD) are depicted as boxes with dashed lines and signal

921 peptide is depicted as a blue box. NP, nucleoprotein; G, glycoprotein; ZnF, zinc-like finger;
922 RdRP, RNA dependent RNA polymerase. **C)** AeAV is a member of the *Anphevirus* genus
923 (red), related to members of the *Nyamiviridae* (pink) and *Bornaviridae* (purple) in an
924 unassigned family within the order *Mononegavirales*. A multiple sequence alignment of the
925 RNA dependent RNA polymerase and the mRNA capping domain was used to create a
926 Maximum likelihood phylogeny. The phylogeny is arbitrarily rooted. 1000 bootstraps were
927 performed and branches with bootstrap values greater than 85% are highlighted. Branch
928 length represent expected numbers of substitutions per amino acid site. Genbank protein
929 accession numbers are Bolahun virus variant 1 (AOR51366.1), Culex mononega-like virus
930 1 (CMLV1) (ASA47369.1), Culex mononega-like virus 2 (CMLV2) (ASA47322.1), Gambie
931 virus (AOR51379.1), Xincheng Mosquito Virus (XcMV) (YP_009302387.1), Borna disease
932 virus (YP_009269418.1), Canary bornavirus 1 (YP_009268910.1), Loveridges garter
933 snake virus 1 (YP_009055063.1), Parrot bornavirus 1 (AEG78314.1), Variegated squirrel
934 bornavirus 1 (SBT82903.1), Midway nyavirus (YP_002905331.1), Nyamanini nyavirus
935 (YP_002905337.1), Sierra Nevada virus (YP_009044201.1), Soybean cyst nematode
936 socyvirus (YP_009052467.1), Farmington virus (YP_009091823.1), Beihai rhabdo-like
937 virus 3 (APG78650.1), Beihai rhabdo-like virus 5 (YP_009333422.1), Beihai rhabdo-like
938 virus 6 (YP_009333413.1), Drosophila unispina virus 1 (AMK09260.1), Hubei diptera virus
939 11 (YP_009337182.1), Hubei orthoptera virus 5 (YP_009336728.1), Hubei rhabdo-like
940 virus 7 (YP_009337121.1), Orinoco virus (ANQ45640.1), Sanxia Water Strider Virus 4
941 (YP_009288955.1), Shuangao Fly Virus 2 (AJG39135.1), Wenling crustacean virus 12
942 (YP_009336618.1), Wenzhou Crab Virus 1 (YP_009304558.1), Wenzhou tapeworm virus
943 1 (YP_009342311.1), Wuchan romanomermis nematode virus 2 (YP_009342285.1).

944 **Figure 2: Conservation of GATA-like Zinc finger (ZnF) domain and small transmembrane**
945 **domain containing protein between tentative members of the *Anphevirus* taxon. A)** Genome
946 orientation of previously discovered viruses within the *Anphevirus* taxon, and **B)** two viruses within
947 a closely related clade. Predicted ORF encoding the ZnF domain is indicated by a black square.

948 Predicted ORFs containing transmembrane domains are indicated by dashed lines. Genbank
949 accession numbers are shown below virus name. NP, nucleoprotein; G, glycoprotein; ZnF,
950 zinc-like finger; RdRP, RNA dependent RNA polymerase. **C)** Alignment of predicted GATA-
951 like ZnF protein sequence (C-X(2)-C-X(17-20)-C-X(2)-C) between three representative strains of
952 AeAV (Miami, USA ; Pune, India; Rabai, Kenya) and predicted ZnF domain proteins from Figure
953 2A and B.

954 **Figure 3. *Aedes anphevirus* (AeAV) *cis*-regulatory elements.** **A)** Location and orientation of
955 predicted *cis*-regulatory element in AeAV indicated by numbered red arrows; downwards indicating
956 genome and upwards arrow indicating anti-genome. **B)** Predicted minimum free energy (MFE)
957 RNA structure of the region surrounding the motif for each element using the RNAfold web server.
958 Colour indicates probability of base-pairing and motif is indicated by the black line. **C)** Sequence of
959 the conserved motif as predicted by MEME as well as location and the statistical confidence of the
960 motif. Sequences are written 3' to 5' and anti-genome motif sequences 1 and 7 are depicted as
961 reverse complement for visual clarity.

962 **Figure 4. *Aedes anphevirus* (AeAV) has worldwide distribution in *Ae. aegypti* laboratory**
963 **colonies, cell lines and wild-caught mosquitoes.** Locations of mosquito collection from RNA-
964 Seq data that were positive for AeAV (Table S1). Points refer to collection sites from American
965 (orange), Asia-Pacific (blue) and African (green) locations.

966 **Figure 5. *Aedes anphevirus* (AeAV) strains have evolved into African, Asia-Pacific and**
967 **American lineages.** **A)** Maximum likelihood phylogeny (PhyML) between AeAV strains using a
968 General Time Reversible (GTR) + G +T model with 1000 bootstraps. Branch lengths represent
969 expected numbers of substitutions per nucleotide site. For visual clarity, the RML-12 clade and
970 Miami clades were collapsed and single examples were shown. **B)** Evolutionary history of
971 worldwide sampling of *Ae. aegypti* adapted from (59, 60) from 1504 SNPs species. Bootstrapped
972 neighbour-joining network based on population pairwise chord-distances from with node support
973 over 90% is shown on relevant branches. New World (American) populations in yellow, and Asia-
974 Pacific populations are shown in light blue. We have truncated the tree and rooted to the *Ae.*
975 *aegypti formosus* (Aef) shown as a red branch.

976 **Figure 6. Genomic context for anphevirus-like insertions into the *Ae. aegypti* genome.** A 21,
977 242nt portion of chromosome 2 depicting anphevirus insertions (red) with predicted ORFs that
978 encode for LTR retrotransposase elements (yellow).

979 **Figure 7. *Aedes anphevirus* (AeAV) is infectious to *Aedes* cell lines but does not replicate in**
980 **Huh-7, Vero and BSR vertebrate cell lines. (A)** RT-qPCR of AeAV genome and anti-genome in a
981 five-day time course in *Ae. aegypti* Aa20 cells, and *Ae. albopictus* C6/36 cells. Error bars represent
982 the SEM of three biological replicates. **(B)** RT-PCR of AeAV genome in a seven-day time course in
983 Human hepatocellular carcinoma cells (Huh-7), African green monkey cells (Vero), Baby Hamster
984 Kidney (BSR). M, Mock infected cells.

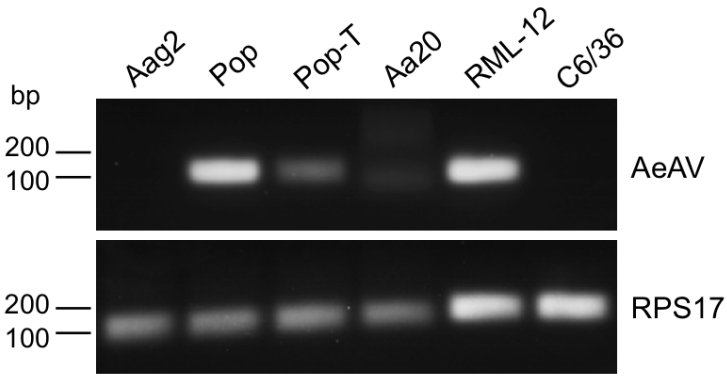
985 **Figure 8. *Aedes anphevirus* (AeAV) genome replication is enhanced by *Wolbachia* infection**
986 **in *Ae. aegypti* cells and produces abundant vsiRNAs and vpiRNAs. A)** RT-qPCR of the AeAV
987 genomic (gRNA) and antigenomic RNA in tetracycline cured Aag2.wMelPop-CLA cells (Pop-tet)
988 and Aag2.wMelPop-CLA cells (Pop) relative to RPS17. Error bars represent the SEM of six
989 (genome) and three (antigenome) biological replicates. n.s, not significant; **, $p < 0.01$. **B)** Mapping
990 profile of pooled small RNA fraction in Aag2.wMelPop-CLA cells. **C)** Alignment of the 21-nt sRNA
991 reads (representing siRNAs), and **D)** the 26-31nt reads (representing piRNAs) mapped to the
992 AeAV antigenome (blue) and genome (red) in Aag2.wMelPop-CLA cells. Relative nucleotide
993 frequency and conservation of the 28nt small RNA reads that mapped to the **E)** genome, and the
994 **F)** anti-genome of AeAV in Aag2.wMelPop-CLA cells.

995 **Figure 9. *Aedes anphevirus* (AeAV) reduces dengue virus replication in Aa20 cells.** Aa20
996 cells persistently infected with AeAV were infected with **(A)** 0.1 and **(B)** 1 MOI of dengue virus
997 serotype 2 (DENV-2). Total RNA was extracted at 0, 1, 3 and 5 days following DENV-2 inoculation
998 and analysed by RT-qPCR. **(C)** RT-qPCR analysis of AeAV persistently infected Aa20 cells
999 infected with 0.1 and 1 MOI of DENV-2 using specific primers to the AeAV genome. Error bars
1000 represent the SEM of three biological replicates. n.s, not significant; *, $p < 0.05$; **, $p < 0.01$.

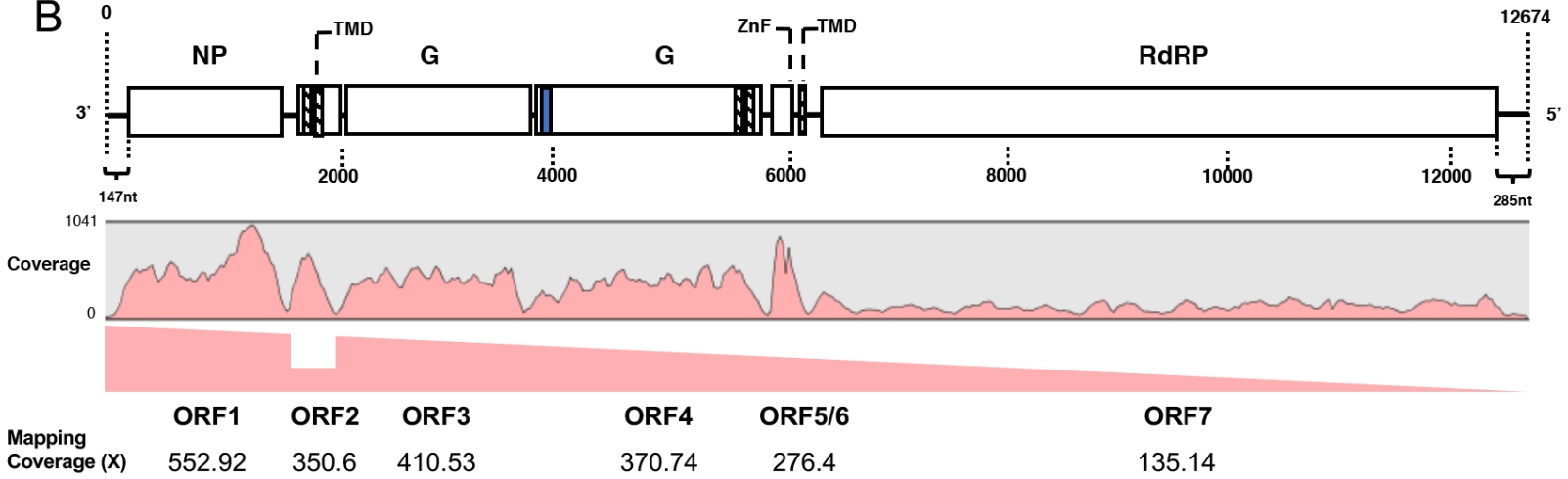
1001 **Figure 10. *Aedes anphevirus* (AeAV) is potentially vertically transmitted. A)** Diagram showing
1002 the parental (K14, K27) and hybrid strains (GP1, GP2, HP1, HP2) from (49). **B)** Table showing
1003 assembly statistics and BLASTN similarity of AeAV assembled from K14 and K27 hybrid strains.

Figure 1

A



B



C

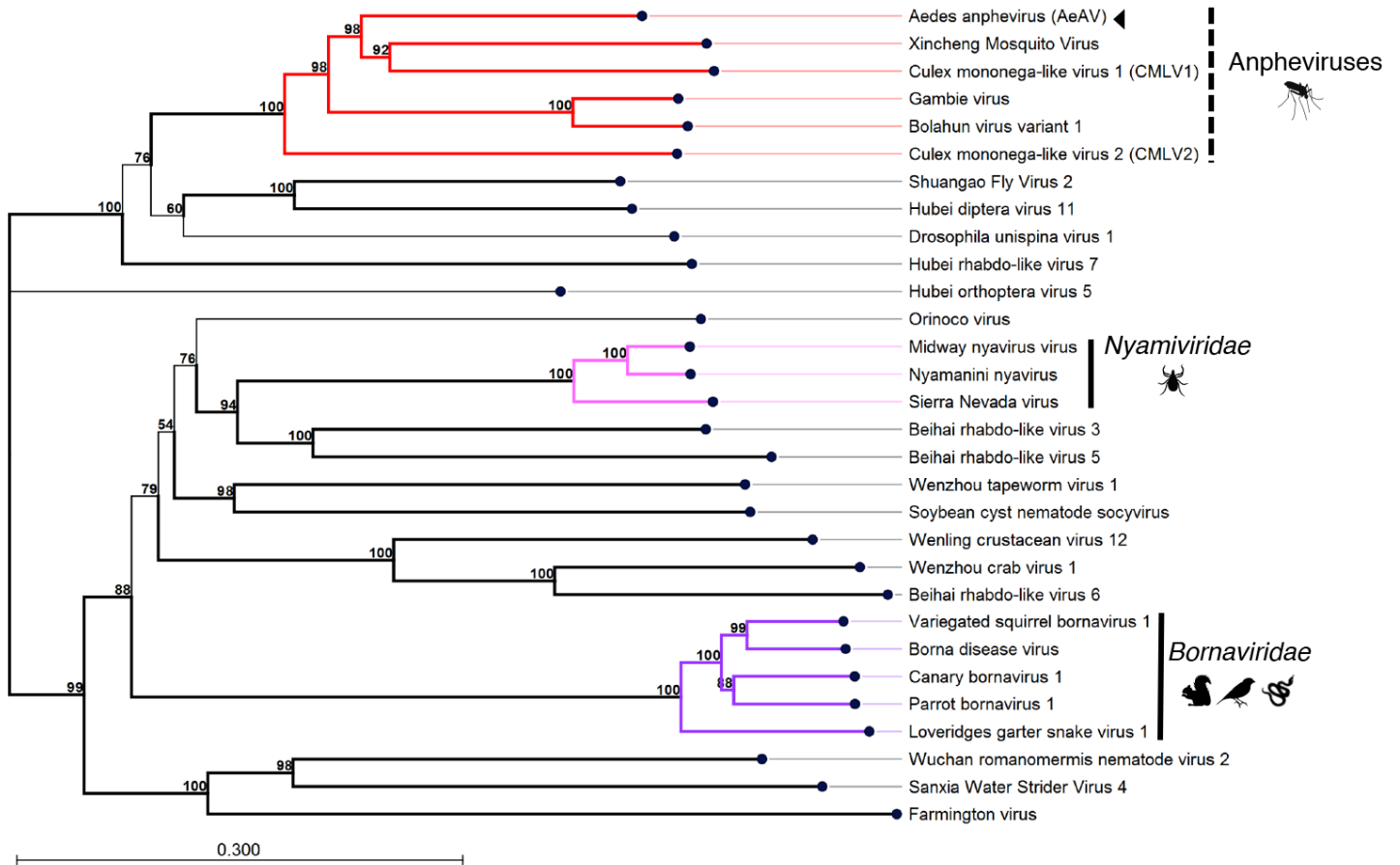


Figure 2

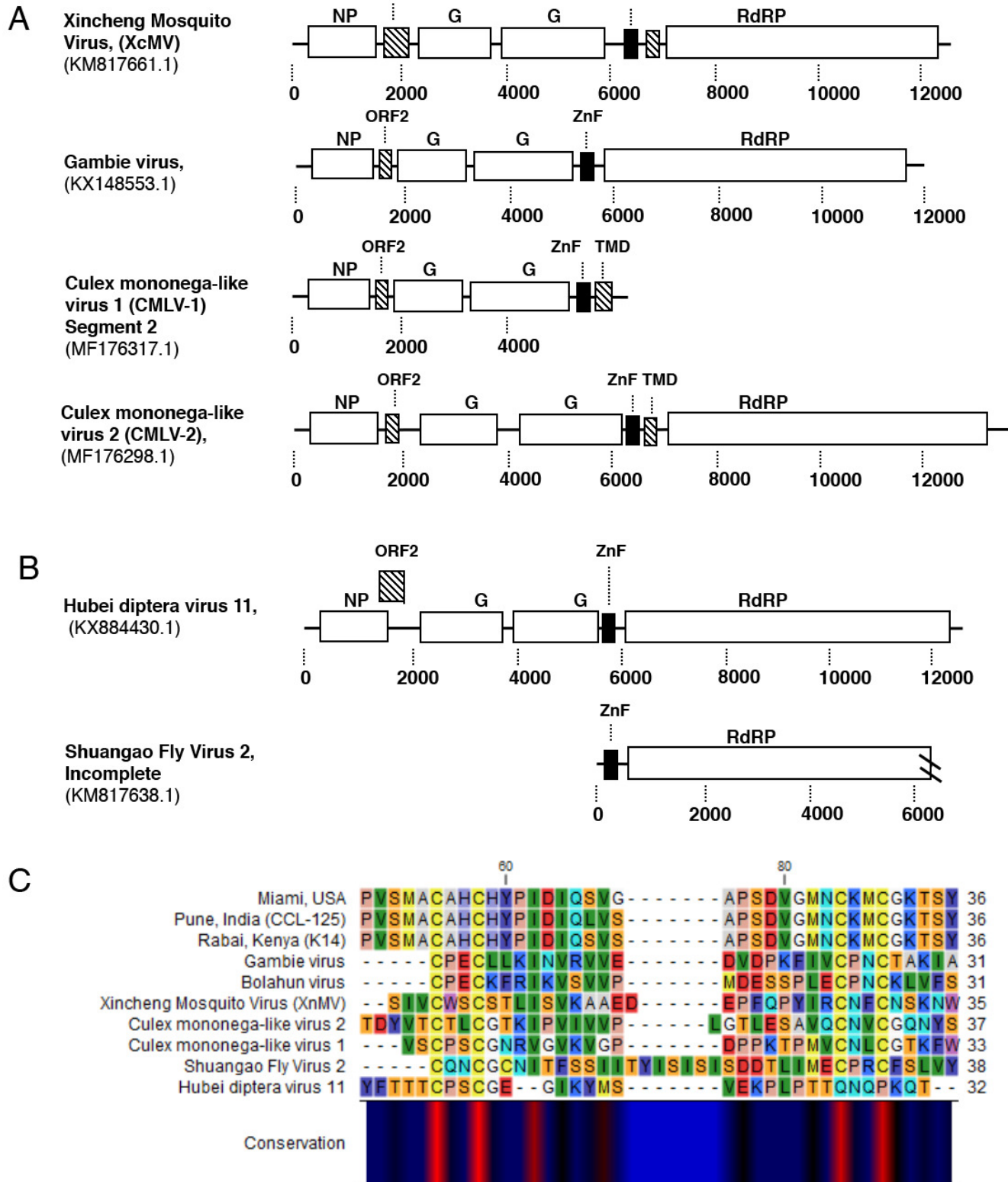


Figure 3

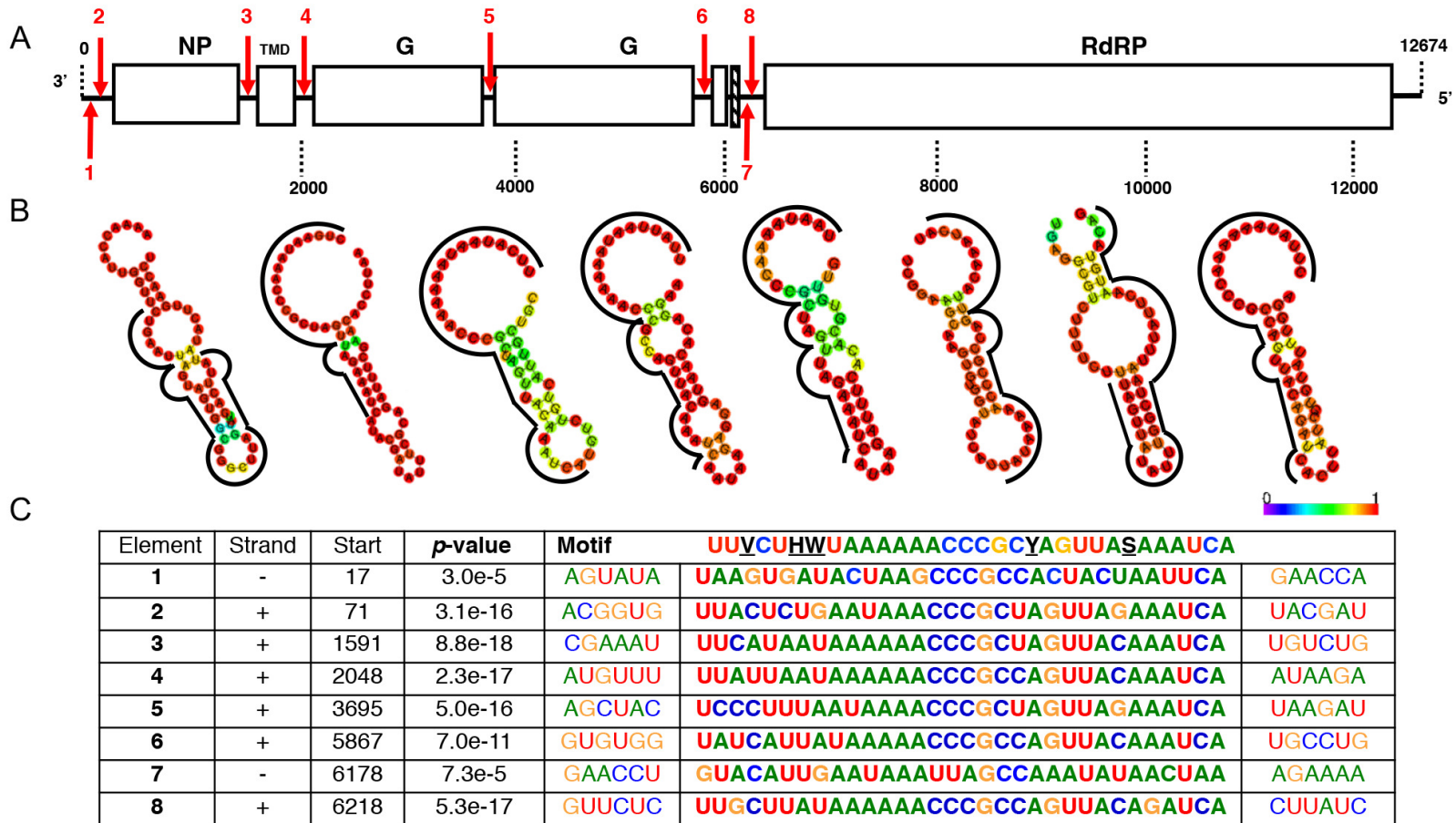


Figure 4

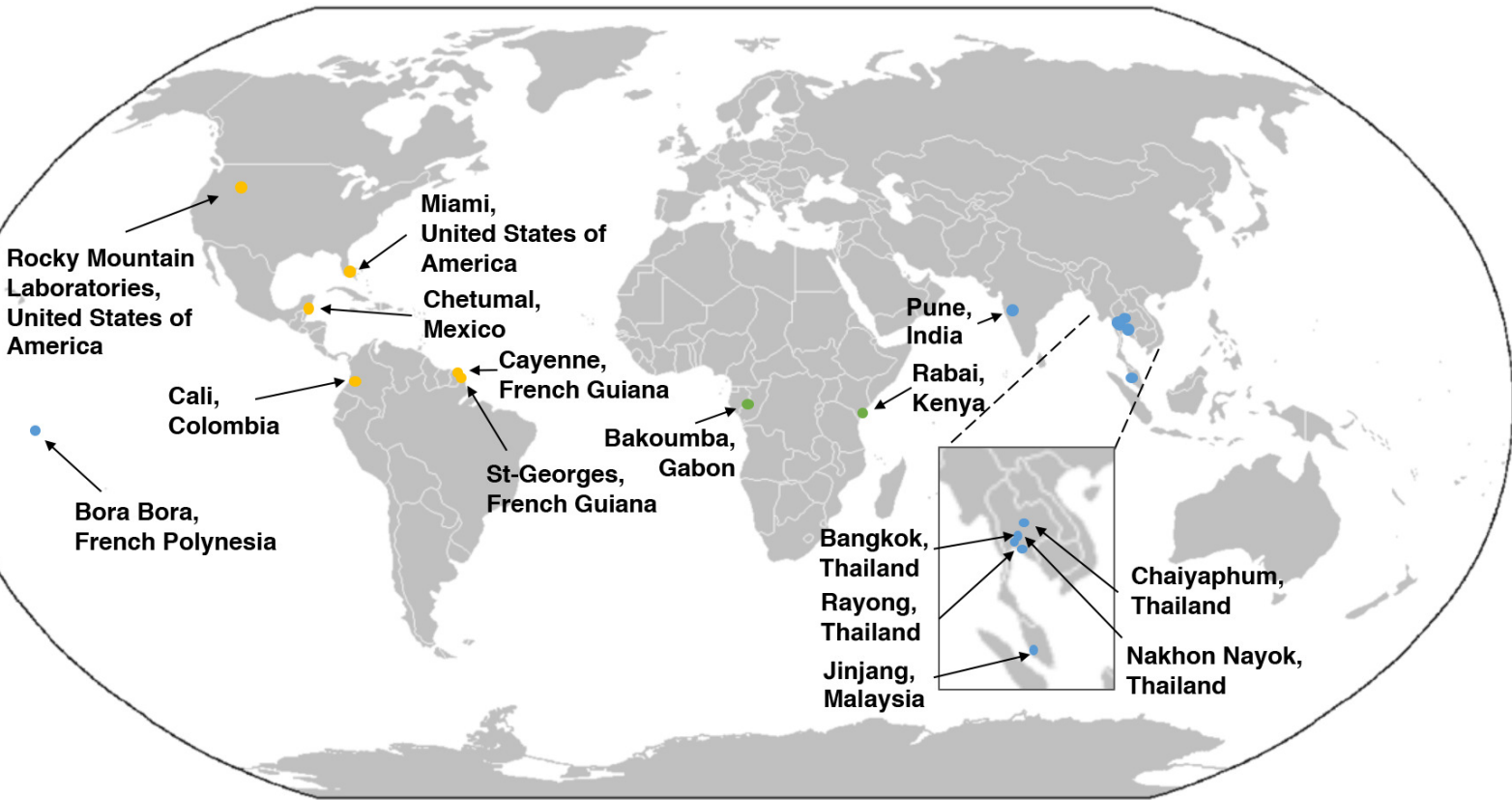


Figure 5

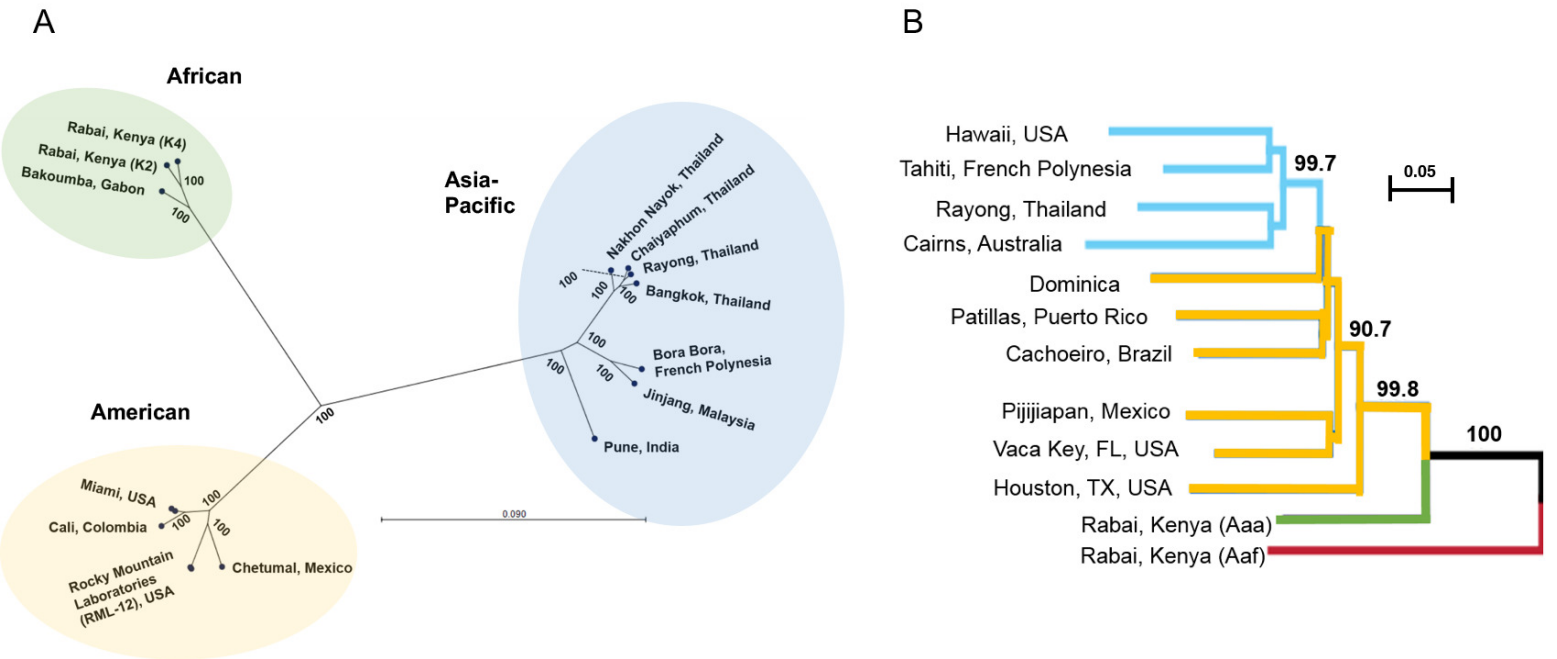


Figure 6

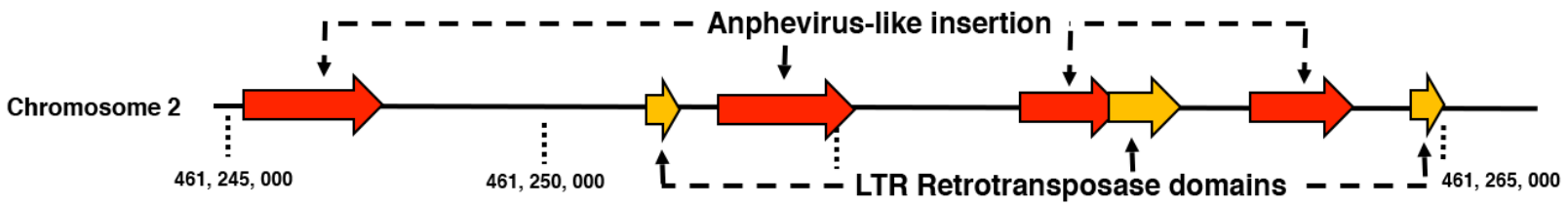


Figure 7

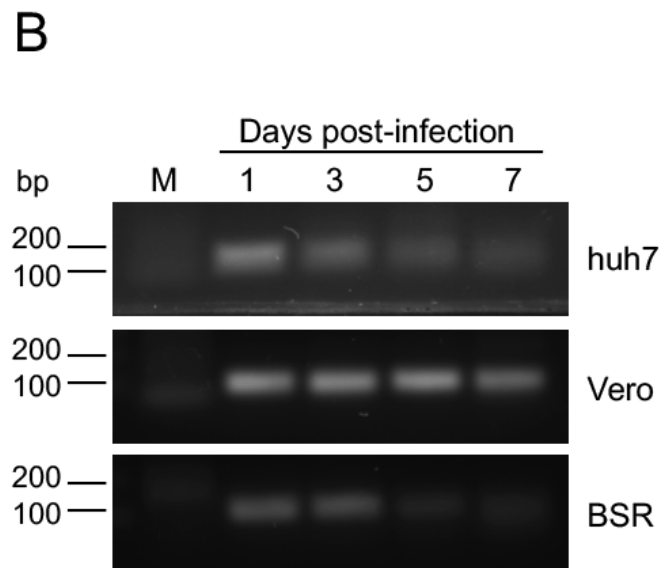
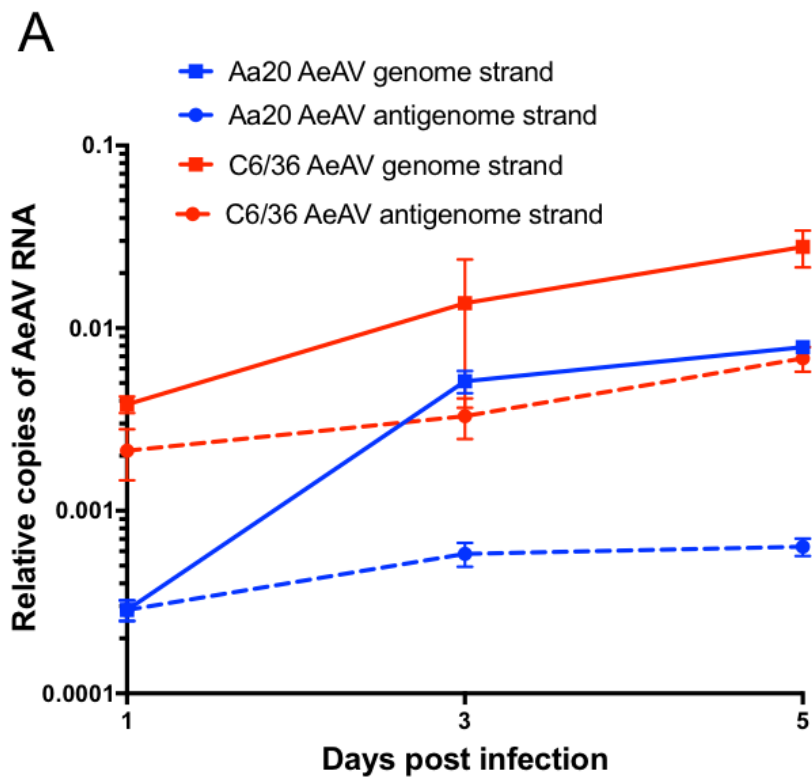
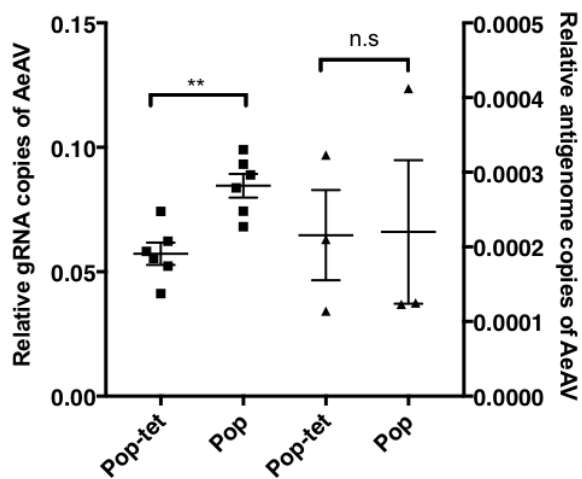
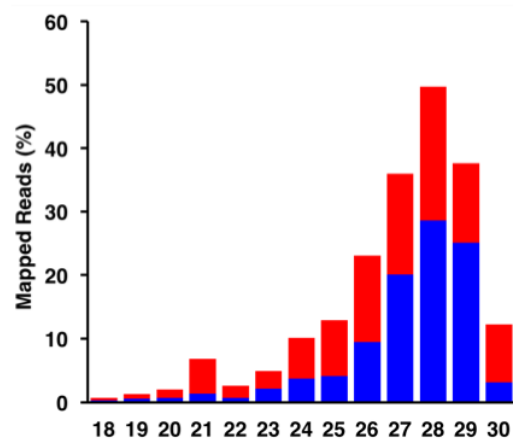


Figure 8

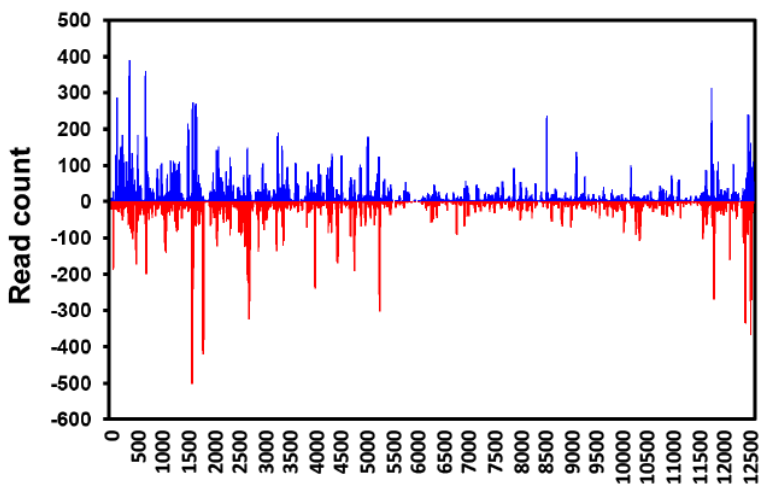
A



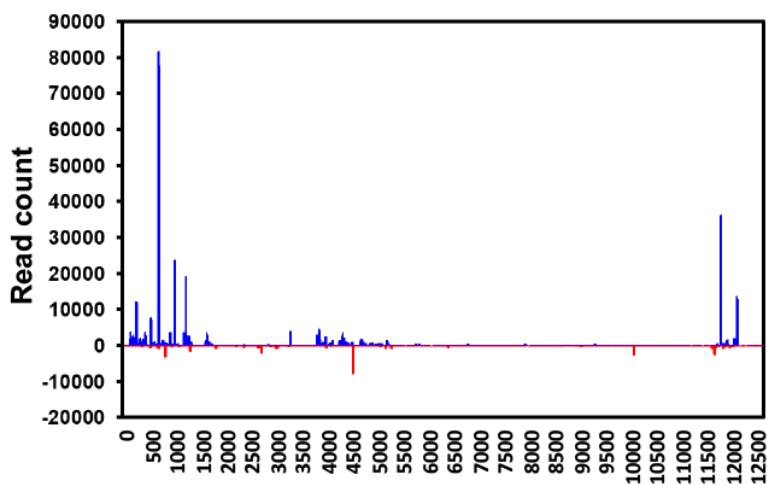
B



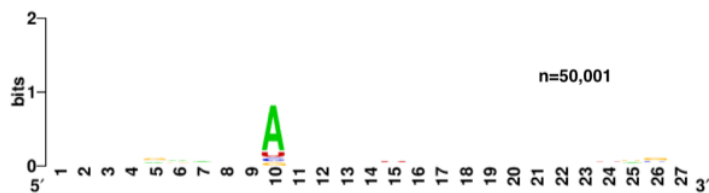
C



D



E



F

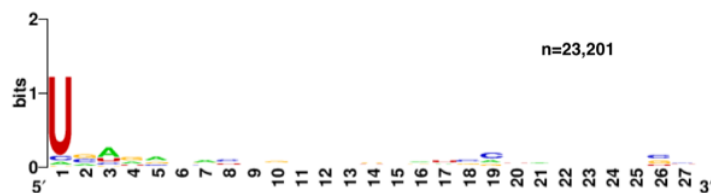


Figure 9

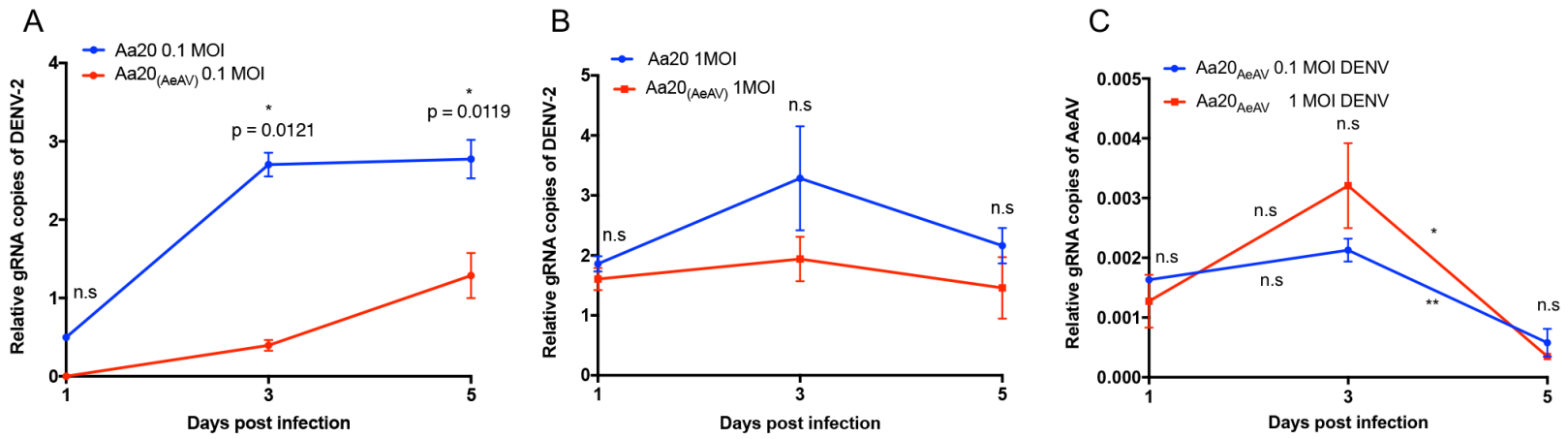
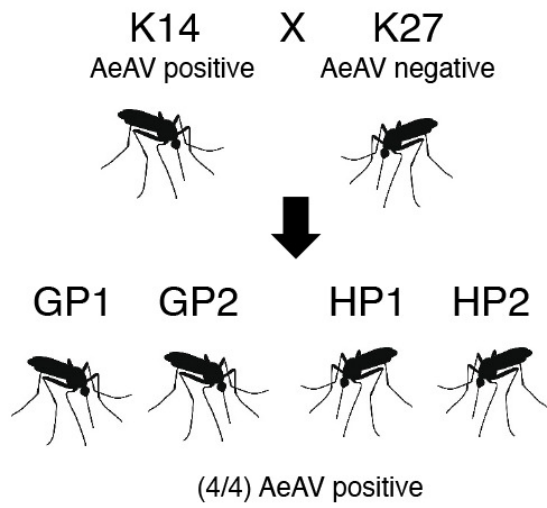


Figure 10



Parental Strains		K14	K27	
Assembled AeAV genome		13,012	-	
Hybrid Strains	GP1	GP2	HP1	HP2
Assembled AeAV genome	13,059	13,034	13,010	7,191; 5,962
BLASTN identity to K14	100%	100%	100%	100%